Advances in Applied Energy 17 (2025) 100207

Contents lists available at ScienceDirect

Advances in Applied Energy

journal homepage: www.elsevier.com/locate/adapen

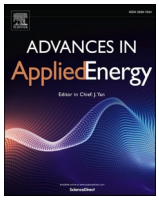

A newly developed spatially resolved modelling framework for hydrogen valleys: Methodology and functionality

Friedrich Mendler [a,b,*], Christopher Voglstätter [a], Nikolas Müller [a], Tom Smolinka [a], Marius Holst [a], Christopher Hebling [a], Barbara Koch [b]

[a] Hydrogen Division, Fraunhofer Institute for Solar Energy Systems, Freiburg, Germany
[b] Chair of Remote Sensing and Landscape Information Systems, University of Freiburg, Freiburg, Germany

ARTICLE INFO

Keywords:
Techno-economic analysis
Optimization
Green hydrogen
Geospatial analysis
Renewable energy sources

ABSTRACT

Regional initiatives, like the European hydrogen valleys, aim to solve the simultaneous absence of green hydrogen production, infrastructure, and application with coordinated development of the whole supply chain. A new model framework was developed to bridge the gap between linearised energy system models and detailed plant simulations that allows for dynamic, nonlinear simulation and optimisation of regional hydrogen systems from electricity generation to hydrogen application. The model incorporates different supply algorithms for electricity and hydrogen, representing both bilateral contracts and flexible markets. A case study demonstrates the application of the framework within a representative hydrogen valley in Germany, showing how the model can identify optimal configurations of hydrogen production, storage, and distribution infrastructure to minimise the levelized cost of hydrogen. The influence of different spatial resolutions, exchange control algorithms, and boundary conditions chain are evaluated. A too coarse spatial resolution can underestimate system cost by up to 10 % while the allowance of both bilateral hydrogen contracts and a flexible market algorithm can increase hydrogen utilisation and reduce cost by up to 15 %. An autarkic supply of hydrogen demands was possible for 7.60 €/kg, while the option to use grid electricity reduces costs to 6.37 €/kg and the option to import hydrogen to 6.60 €/kg, based on the assumptions for electricity and hydrogen prices. This work contributes to the evolving field of hydrogen economy by providing a sophisticated tool for policymakers and industry stakeholders worldwide to plan and optimise regional hydrogen valleys effectively.

1. Introduction

While there is scientific and political consensus that hydrogen will play a key role in the full defossilisation of energy systems worldwide [1], the simultaneous lack of (green) hydrogen production, hydrogen infrastructure, and hydrogen consumers willing to pay the difference to fossil hydrogen impedes the development of the hydrogen economy. Regional initiatives, commonly labelled as “hydrogen valleys”, have formed to coordinate and harmonise the development of the different parts of the hydrogen supply chain (HSC). Bampaou et al. [2] recently published a non-exhaustive global overview of hydrogen valleys in different development stages. Although the majority of the listed projects are in Europe, hydrogen valleys are established on nearly all other continents as a map by the Clean Hydrogen Partnership shows [3]. The United States supports the development of hydrogen valleys with $8 billion within their Regional Clean Hydrogen Hub program, the “the largest federally funded deployments of clean hydrogen technologies in the United States” [4]. Hydrogen valleys further play a crucial role in the

Abbreviations: AES, Alternative electricity sources; BCT, Between cluster transport; BEC, Bilateral electricity contracts; BHC, Bilateral hydrogen contracts; BOP, Balance of plant; CAPEX, Capital expenditures; CMA-ES, Covariance Matrix Adaptation Evolution Strategy; ESOM, Energy system optimisation model; FLH, Full load hours; HEA, Hydrogen exchange algorithm; HRS, Hydrogen refuelling station; HSC, Hydrogen supply chain; HYSCOPE, Hydrogen Supply Chain OPtimization Engine; ICT, Intracluster transport; KPI, Key performance indicator; LCOH, Levelized cost of hydrogen; LP, Linear problem; m, hydrogen mass; MILP, Mixed integer linear problem; NLP, Nonlinear problem; OEMA, Open electricity market algorithm; OPEX, Operational expenditures; Opt, Optimisation; PV, Photovoltaic; RE, Renewable electricity; SCHC, Spatially constrained hierarchical clustering; Sim, Simulation; SURR, Southern upper rhine region; TEOM, Techno-economic optimisation model; WPP, Wind power plant.

* Corresponding author.
E-mail address: friedrich.mendler@ise.fraunhofer.de (F. Mendler).

https://doi.org/10.1016/j.adapen.2025.100207
Received 30 October 2024; Received in revised form 1 January 2025; Accepted 4 January 2025
Available online 5 January 2025

national hydrogen strategies of Australia [5], Canada [6], Germany [7], France [8], Spain [9]and the Netherlands [10]. The optimal design of the HSC in each region depends on many local factors. These include the location and type of major industries, political support and local funding, existing infrastructure, and geographical conditions [11]. As regional hydrogen transport and hydrogen storage can be a major cost driver for hydrogen valleys – especially for small- to mid-scale implementations – an optimal spatial design can have a major impact on the economic feasibility and success of hydrogen valleys. Therefore, a model framework with detailed spatial resolution and realistic representation of spatial relationships is necessary.

There are various energy system optimisation models (ESOM) available that model different levels of spatial and temporal resolutions as well as technological detail. Models that include hydrogen and other parts of the Power-to-X value chain are,i.e., PyPSA [12], REMod [13], TIMES [14], and EnergyScope [15]. Aryanpur et al. [16] provide a comprehensive review of different ESOMs and their spatiotemporal resolution and conclude that they "can permit regional disaggregation up to the first-level administrative divisions within a country (such as state and province) while maintaining computationally tractable". This regional scope, together with their usual implementation as linear (LP) or mixed-integer linear problems (MILP), limits their applicability in the modelling of hydrogen valleys with high spatial and technical detail. Sahoo et al. developed an adaptation of the ESOM OPERA [17] for regional analyses and applied it in the northern Netherlands [18] and on Groningen [19], but only implemented a simplified hydrogen system with a higher focus on district heating. ESOMs with a more detailed representation of hydrogen technologies have been developed by Ball et al. [20] and Welder et al. [21]. Both models have a larger spatial extent and a lower spatial resolution, with federal states of Germany representing nodes and limited technical detail being formulated as MILP. Furthermore, [21] is limited to optimising representative days instead of a full year in hourly resolution to reduce the number of operational decision variables. As seasonal differences in renewable energy production and therefore renewable hydrogen production have a big impact on the supply, storage, and thereby costs of the HSC, this limits the significance of these results for hydrogen valleys.

Besides the spatially explicit ESOMs, techno-economic optimisation models (TEOM) exist that focus more on technical detail, like the modelling framework H_2ProSim developed at Fraunhofer ISE. These studies are usually lacking a spatial resolution as a trade-off for higher technical detail and more flexible operation in nonlinear problems (NLP), like the optimisation model developed by Hou et al. [22]. Another TEA without spatial dimension has been performed for multiple locations on European islands for hydrogen production for different electricity supply scenarios [23] and one by Petrollese et al. for a case study in Cagliari, Italy, showing the benefits from having different flexible hydrogen consumers [24].

Spatially explicit TEOMs have also been established in the literature for many years but are subject to various limitations. They can be clustered in models with high spatial and technical resolution but no dynamic simulation and models with dynamic processes modelled with temporal resolution (usually hourly) that are usually implemented as MILP. An overview of the most relevant literature applying models of the first group can be found in Appendix Table 1 and Appendix Table 2 for the second group. Early approaches of the first group consist of studies by Konda et al. [25], De-León et al. [26,27], Parker et al. [28], and André et al. [29]. All studies apply models with high spatial resolution to analyse realistic pipeline networks and truck routing routines. The latter two formulated even an NLP to include realistic techno-economic pipeline representation. De-León et al. applied an MILP model on different spatial scales in [26] and [27], demonstrating difficulties, especially from differences in input data. Newer studies of the first group even increased the spatial detail. Talebian et al. [30] included another spatial resolution level for hydrogen distribution and, Forghani et al. [31] implemented a pipeline routing network, instead of only point-to-point pipeline transport as implemented in most other models. Cantú et al. [32] combine an MILP with an NLP to achieve a multi-objective optimisation of both hydrogen cost and greenhouse gas emissions. Li et al. [33] used Markov Chain analyses to compare the sustainability of investments resulting from the MILP optimisation of different scenarios. These proved the superiority of electrolysis in long-term planning above other hydrogen production technologies. Guzzini et al. [34] combined a high spatial resolution with discrete plant sizes for production and hydrogen refuelling stations (HRS) to improve the representation of these technologies within the model. Cutore et al. [35] analyse the potential of using the existing wind power plants (WPP) for hydrogen production in Sicily, Italy. Pérez-Uresti et al. [36] combine detailed plant simulation in different environments of the *Aspen* software with an NLP optimisation to implement realistic plant behaviour and to differentiate between hydrogen purity levels on consumer sites. All the aforementioned studies of the first group share the limitation that fluctuations in production and demand, especially coming from RE production, cannot be considered in the static model approach. Therefore, the question of electricity and hydrogen production sources is analysed in less detail. Interestingly, all of the studies of the first group only considered HRS as potential hydrogen demand sites. The only exception is Pérez-Uresti et al., which differentiates between HRS and industrial hydrogen applications and the respective level of necessary hydrogen purity.

The models found in literature that seem the most fitting to the problem addressed in this work are part of the second group of models. They are listed in Appendix Table 2 and all include a dynamic modelling of a spatially resolved HSC. Part of this group are the approaches by He et al. [37] and Wang et al. [38], with the latter being an extension of the first. He et al. [37] are presenting a MILP with hourly-resolved simulation of 20 representative weeks for the US Northeast subdivided into six

Table 1
Modelling scenarios grouped by the main question to analyse.

Number	Name	Description	Number of clusters (after excluding clusters of no interest)
1	CL5	REDCAP for 5 clusters	5
2	CL10	REDCAP for 10 clusters	10
3	CL20	REDCAP for 20 clusters	20
4	CL30	REDCAP for 30 clusters	30
5	CL40 (base)	REDCAP for 40 clusters	38
6	CL50	REDCAP for 50 clusters	46
7	CL60	REDCAP for 60 clusters	54
8	CL80	REDCAP for 80 clusters	66
9	CL20_SCHC	SCHC for 20 clusters	20
10	CL40_SCHC	SCHC for 40 clusters	38
11	CL80_SCHC	SCHC for 80 clusters	68
12	BHC	H2 transport only via BHC	38
13	Pull	H2 transport only via Pull	38
14	BHC + Push	No Pull H2 transport	38
15	BHC + Pull	No Push H2 transport	38
16	Push + Pull	No BHC H2 transport	38
17	Grid Elec	Grid electricity allowed	38
18	Import	H2 import allowed	38
19	Export	H2 export allowed	38
20	Import & Export	H2 import and export allowed	38

Table 2
Selected results for scenario group I. For low resolution, higher amounts of AES are used, as average RE FLH are lower and more hydropower plants can be used in one cluster. Results are relatively similar from CL30 to higher resolution.

Result	Unit	CL5	CL10	CL20	CL30	CL40	CL50	CL60	CL80
LCOH	€/kg	7.04	7.38	7.96	7.67	7.60	7.64	7.62	7.87
# Ely	-	3	6	12	13	12	14	12	12
$E_{RE,total}$	GWh	2405	2842	3342	2927	2850	2790	2837	3087
$E_{AES,total}$	GWh	1097	828	540	660	765	784	778	596
$FLH_{PV,mean}$	h	1135	1145	1177	1186	1186	1191	1181	1184
$FLH_{WPP,mean}$	h	1595	1868	2070	2345	2408	2356	2449	2330
$r_{elec,trans}$	-	0.02	0.16	0.26	0.55	0.43	0.47	0.43	0.65
$r_{H2,trans}$	-	0.50	0.76	0.79	0.62	0.94	0.77	0.95	0.55
Sim time	s	5.14	6.46	9.96	15.72	22.12	27.82	35.01	51.52
# Opt runs in one job	-	10	10	10	5	4	2	1	1

zones. The transport technologies – truck trailers and pipelines – are both modelled for transport and mobile storage which reduces demand for stationary storage by more than 70 %. RE is not included in the study but only grid electricity combined with a power price, and even though the model is formulated as MILP, integer variables (especially truck numbers) are simplified to solve it as LP to reduce computing time. Wang et al. [38] expand this approach by integrating fluctuating wind electricity and power transmission lines. Another MILP has been applied by Parolin et al. in Sicily [39]. Although this approach has a very high spatial detail with a total of 98 nodes, it has only limited dynamics and representation of RE with a daily temporal resolution. The same can be said regarding the study by Genovese et al. [40] in Calabria, which includes not an optimisation but the simulation of multiple setups. Another analysis of the operation of a spatially resolved HSC has been conducted by Rosén et al. [41], who applied a regional energy system model on a three-node Hydrogen Valley in Western Sweden. The results show that hydrogen pipelines can be beneficial for the whole energy system by reducing total cost by 4–7 %. All models of the second group are linearised towards a MILP, reducing the level of technical detail.

Summarising the literature research, there is no existing, spatially explicit, nonlinear, and dynamic modelling approach for HSCs. This work aims to address this gap and provides a solution and analyses the reliability and computational solvability of the problem. Besides a spatial resolution, the model framework needs high technical, economical, and temporal resolution to be applicable on a small scale and assess the influence of single stakeholders or projects that typically have a high impact in the region. ESOMs that are usually built on a linear framework with low spatial resolution to simulate national or supernational energy systems reach their limits here. A spatially explicit technical system analysis can bridge this gap of model applicability. For this, the *Hydrogen Supply Chain OPtimization Engine* (HYSCOPE) was developed and will be published for the first time in full functionality in the scope of this work. It is intended to close the research gap of integrated HSC optimisation on a regional scale by combining approaches of both ESOMs and TEOMs, as visualised in Fig. 1. The application of HYSCOPE aims to answer the most important questions regarding an optimal hydrogen system with respect to the local conditions like the following:

- Decentralised systems to reduce transport efforts or centralised hydrogen generation to take advantage of economies of scale?
- Which transport technology is best under which boundary conditions? Power lines for electricity or pipelines, trailers, or rail transport for hydrogen?
- Which electricity sources and electrolysis operations offer the lowest hydrogen production cost?
- Where are the break-even points for local production compared to import options?

In the following section, ISE's model framework H_2ProSim is briefly described as the basis for HYSCOPE. Afterwards the clustering process that creates the spatial resolution is presented. The main part of this study focuses on the spatial augmentation of H_2ProSim, including all newly implemented algorithms and technologies for a spatially resolved HSC. Afterwards the newly developed model is applied to one representative hydrogen valley in Germany to show the potential of

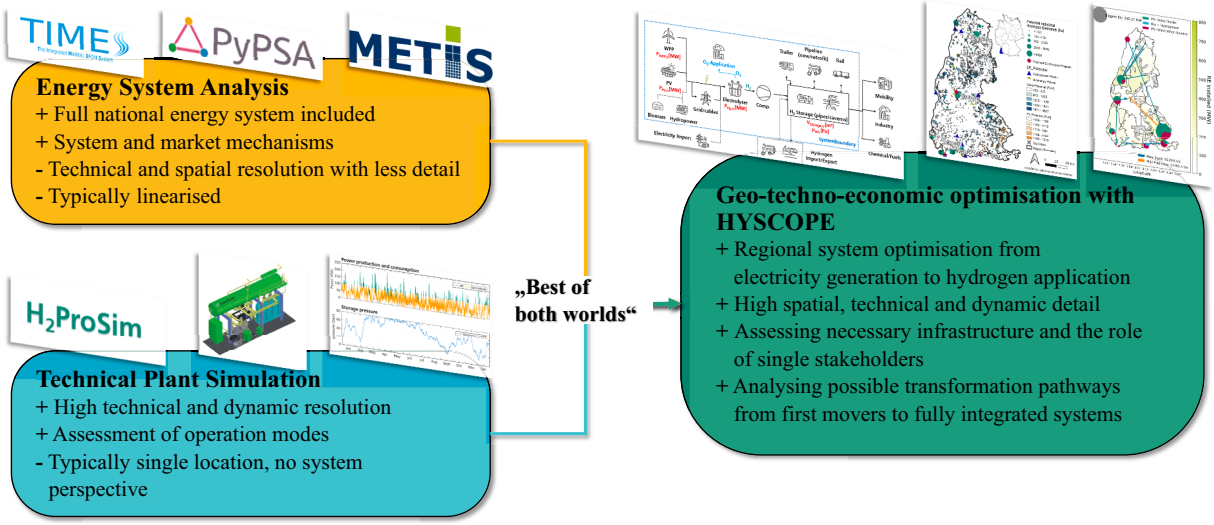

Fig. 1. Significance of the proposed modelling environment to close the scientific gap between energy system analysis and plant simulations by combining the strengths of both fields.

HYSCOPE and verify its functionality. The results are evaluated with respect to hydrogen strategies around the world. The work concludes with a critical discussion of the model framework, existing limitations, and possible improvements in further research.

2. Methodology

In this chapter the spatially resolved optimisation model for HSCs is described. The HSC is presented first to give an overview regarding all included technologies. The model is based on the modelling framework H_2ProSim [42], which is embedded in a model chain to handle spatial data. After a brief description of both and the methodology for deriving the spatial resolution, the functionality of the newly developed spatially resolved model is presented in detail. This includes a description of the optimisation framework, algorithms controlling the operation of the HSC, and the system for economic evaluation of the simulation results. The methodology chapter concludes with a description of the case study that is modelled for the result section.

2.1. Hydrogen supply chain

In the scope of this work, the full HSC from electricity production to hydrogen application is analysed in the optimisation model. Electricity is primarily sourced from newly built, dedicated photovoltaic power plants (PV) and WPP. In specific scenarios, the use of alternative electricity sources (AES) in times of low RE output is allowed, either from local hydropower or bioenergy plants or from external grid electricity. Costs for alternative electricity are based on the fluctuating electricity prices at the stock market. After production, the electricity can be directly fed into the electrolysis or transported via power lines within the hydrogen valley. Similarly, the hydrogen produced by electrolysis can be directly fed into the application, stored locally, or transported to other subregions of the study region via different transport technologies. Based on the scenario, the byproduct oxygen can be used on-site for additional revenues, and/or hydrogen can be imported/exported from/to outside the region at suitable exchange points. The full value chain is depicted in Fig. 2 with the decision variables and their units highlighted in red (Further details in the section Decision Variables).

2.2. Model environment H2ProSim

In the scope of this work, Fraunhofer ISE's simulation and optimisation environment H_2ProSim [42] is extended regarding a spatial dimension. H_2ProSim allows dynamic, nonlinear, and modular simulation of the full HSC from electricity generation to hydrogen application. The general modelling workflow of H_2ProSim is shown in Fig. 3. The simulation is typically embedded in a nonlinear techno-economic optimisation via Covariance Matrix Adaptation Evolution Strategy (CMA-ES) to optimise plant setup and operation. The model framework is built in *Matlab,* while the technical simulation is performed in *Matlab's* simulation environment, *Simulink*. The model allows for a hydrogen plant simulation including load-dependent efficiencies, ramp-up phases, real gas behaviour, and nonlinear control algorithms for electricity supply. All these advantages of the nonlinear framework are inherited by HYSCOPE. A predefined time, typically a representative year, is simulated in high temporal resolution, which can range from seconds to hours. In the scope of this work, a 30 min timestep is used for simulation while the results are evaluated every hour. The simulation results are further processed in an economic model to derive the levelized cost of hydrogen (LCOH) and other key performance indicators (KPI) while respecting non-linear cost-degressions and component-specific lifetimes. In H_2ProSim, operational decisions like the operation of the electrolysis plant are determined through algorithms within the simulation that are dependent on planning decision variables and manually defined parameters. For further description of H_2ProSim and the technical modelling approach, see [42].

2.3. Spatial resolution and clustering

For the presented modelling framework the spatial clustering is performed via "regionalization with dynamically constrained agglomerative clustering and partitioning" (REDCAP) [43] as a base case and compared to spatially constrained hierarchical clustering (SCHC). The clustering variables are the hydrogen demand locations, including the pre-optimised HRS network and the different RE sources. The results from clustering the case study analysed in this work, the Southern Upper Rhine Region (SURR), for 40 clusters can be seen in Fig. 4. Each cluster is assigned a role based on its most important characteristic, which is also used to determine the weighted centroid. The cluster role is represented

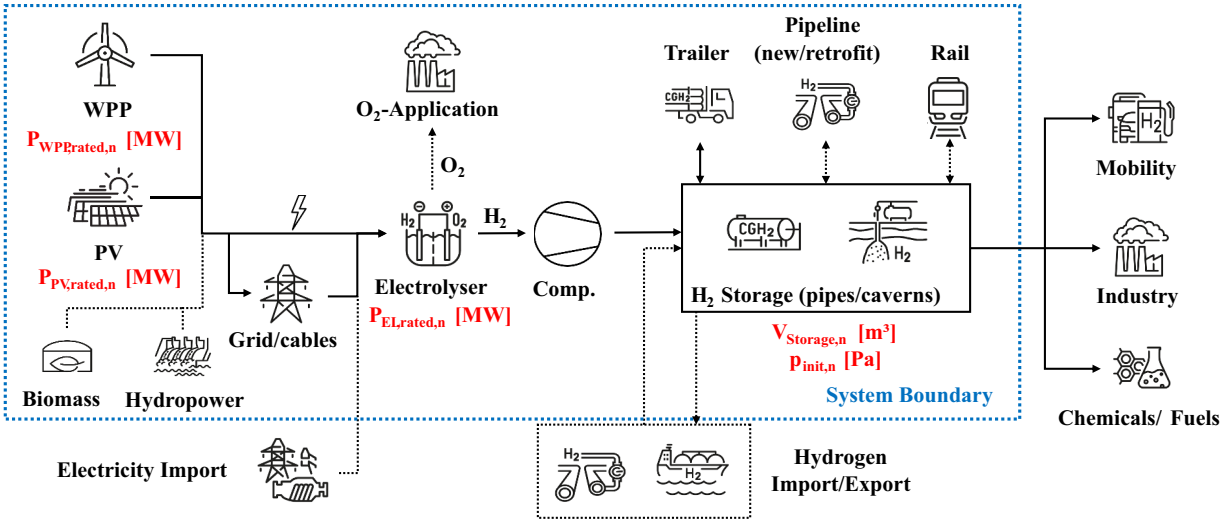

Fig. 2. Modelled hydrogen supply chain, including the decision variables displayed in red. Scenario-specific technologies are marked with dashed lines. The system boundary is marked as a blue dashed rectangle.

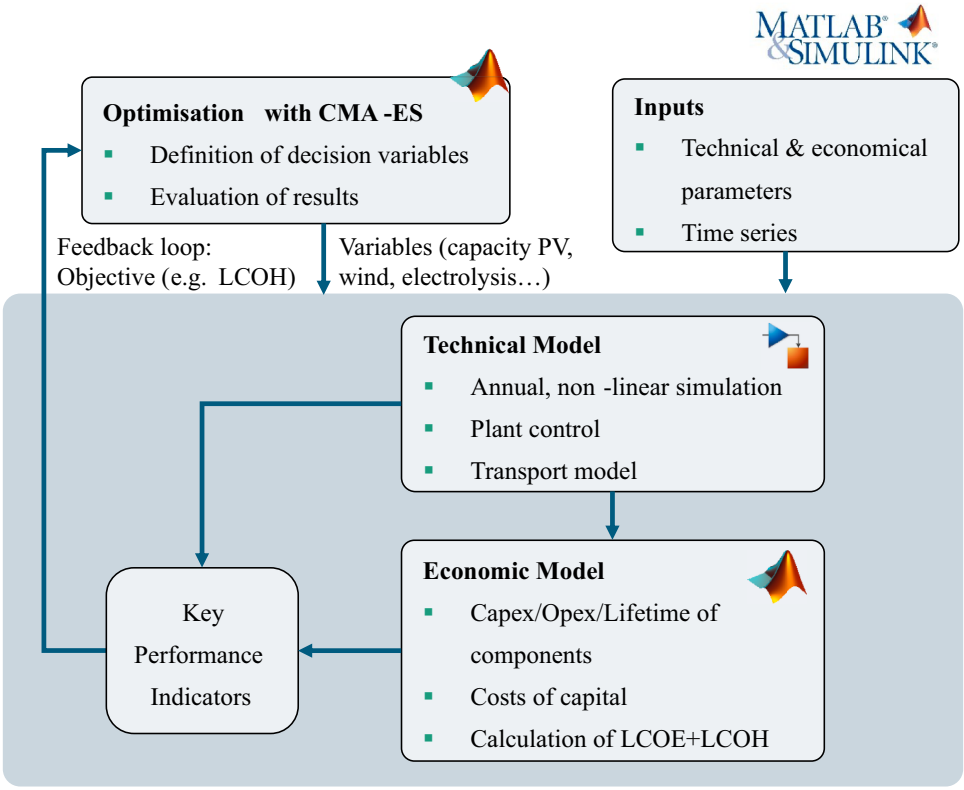

Fig. 3. H_2ProSim optimisation workflow that is also used for HYSCOPE. Technical simulation in SIMULINK and economic evaluation are performed in every iteration of the optimisation algorithm.

by the background colour and the weighted centre is marked with a cross. If a cluster has no role because it has neither hydrogen demand nor RE potential, it is excluded before optimisation to reduce complexity. This is visible in Fig. 4 by the white spots on the map and a total of 38 clusters. Further details on algorithm selection and parametrisation can be found in previous work of our group [44].

Each cluster is represented by a node in HYSCOPE. Inputs of the optimisation model can be divided into intracluster parameters (vectors) and intercluster parameters (matrices). The first summarises the conditions within each cluster, like RE installation potential, hydrogen demand, or connection capacities to grids. The intercluster matrices describe the connections between clusters, like travel distances along different transport modes or possible transport infrastructure.

2.4. The Optimisation Framework

2.4.1. Decision Variables

The decision variables are depicted within the HSC in Fig. 2 in red font. Following the nodal structure of HYSCOPE, the decision variables that have been scalars in the standard H_2ProSim environment are now represented as vectors with one entry for each node. This applies to the following variables:

- PV capacities $\boldsymbol{P}_{PV,rated,n}$
- WPP capacities $\boldsymbol{P}_{WPP,rated,n}$
- Electrolysis capacities $\boldsymbol{P}_{EL,rated,n}$
- Hydrogen storage volume $\boldsymbol{V}_{storage,n}$
- Hydrogen storage initial pressure $\boldsymbol{p}_{init,n}$

All variables are limited by upper bounds that are usually determined by geographical conditions like the available area for RE installations or potential storage volumes, which can depend on geological conditions and sufficient space for overground or underground installation. Usually, the system is modelled as a greenfield approach, so the lower boundary for plant capacities is zero. Minimum plant sizes for installation are realistic, therefore, in the scope of this work, decision variables for electrolysis smaller than 5 MW are set to zero. If a plant is already installed or an installation is planned, the lower boundary can be set to the desired value.

As usual for H_2ProSim, no operational decision variables are used in optimisation to keep the NLP computationally tractable. Instead, the operation of the plants and the exchange of electricity and hydrogen are controlled at each timestep through distinctive algorithms. The plant operation control is presented in [42], while the exchange algorithms are newly introduced in the scope of this work and presented in the section Control Algorithms.

2.4.2. Boundary Conditions

The most important constraints are the spatiotemporally resolved hydrogen demands that need to be met at each location and timestep. If a demand cannot be supplied, an artificial penalty is added to the total cost. Therefore, the optimisation algorithm avoids plant setups leading to insufficient supply and guarantees the fulfilment of hydrogen demand. Further boundary conditions include the aforementioned intracluster parameters, which can be implemented as direct bounds for decision variables (like RE potential) or implemented as an individual limit in the simulation. Examples for the latter are local import capacities for electricity or hydrogen or installed hydropower capacities. The last group of boundary conditions are timeseries for the specific RE production and the price for buying external electricity as AES. The RE timeseries are derived from the *Photovoltaic Geographical Information System* [45] for each node. The specific RE output of 2015 has been chosen as this was a year in Germany with historically average weather conditions for the production of PV and WPP electricity. The electricity price timeseries has been taken from SMARD [46]. The power prices at the German stock market from 2015 have been selected to match the

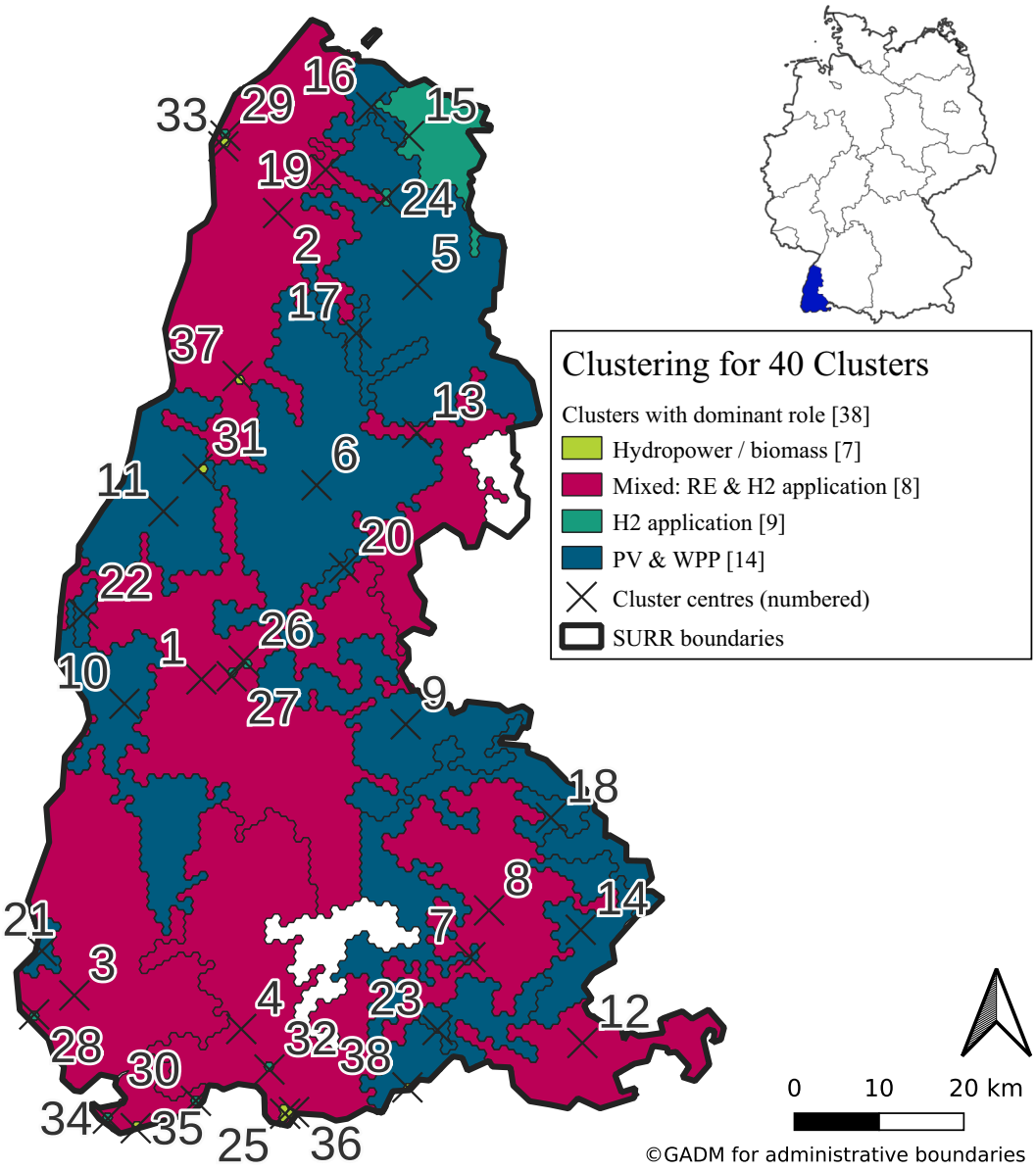

Fig. 4. Results for clustering the case study SURR for 40 clusters with REDCAP. Weighted centroids are displayed as crosses with cluster numbers. The most important characteristic of each region is displayed through its background colour. The distribution of roles is relatively even, but the sizes differ substantially. Clusters formed on H2 applications, hydropower, and biomass are mostly single hexagons (points of high interest), while clusters for RE and mixed clusters take up the majority of the total area.

temporal patterns of RE production curves, as stock market prices are strongly influenced by RE production. To take respect to the recent electricity price development since then, the 2015 timeseries was linearly scaled to the average of 2023 in Germany.

2.4.3. Optimisation algorithm

As already presented in section Model Environment H2ProSim, the analysis of the hydrogen region is performed through nonlinear simulation-based optimisation. Due to the spatial resolution of the decision variables and many potential spatial layouts of the HSC, the solution space is high-dimensional, non-convex, and filled with many local optima. An algorithm that has been shown to be capable of solving algorithms like this is CMA-ES [47]. The distinctive feature of the CMA-ES lies in the adaptation of the covariance matrix, which describes the pairwise interdependencies of the decision variables. This provides a second-order model of the fitness function and is comparable to approximating the inverse Hessian matrix in classical convex quadratic optimisation [48]. The algorithm proved to be faster and more reliable for non-convex and non-linear optimisation than many other optimisation strategies [47]. CMA-ES was first introduced by Hansen and Ostermeier in [49] and continuously improved by the working group of Hansen. To reduce the risk of finding only a local optimum that is substantially worse than the global, several independent restarts of respective setups are recommended for each scenario. Automated triggering of several independent restarts is implemented in the model. In CMA-ES the bounds for all decision variables need to be the same; therefore, box constraints of 0 and 1 are used. These decision variables are transformed linearly with the actual lower boundary (lb) and upper boundary (ub) (see Section 2.4.1) for the simulation according to Eq. (1). Besides box constraints, no constraints are used in CMA-ES. The only

parameters that need to be set in CMA-ES are the starting point and the initial step size. For the starting point, 0.5 is used for all decision variables, as this proved to provide the best results in similar models [50], and for the initial step size 0.3 is used as recommended by the developer of the algorithm [51].

$$x_{sim,i} = lb_i + (ub_i - lb_i)^* x_{CMA-ES,i} \quad (1)$$

In the scope of this work, only single-objective optimisation towards minimal LCOH is performed. LCOH has the advantage of including both the quantity of hydrogen production and the total system costs. For details of the LCOH calculation, see section Economic Evaluation.

2.5. Control algorithms

Following the approach of avoiding operational decision variables, the simulation is solely based on distinct control algorithms that are influenced by the planning decision variables. The simulation can be separated into an electrical and hydrogen part, which will be presented in the following. All steps are performed at each timestep. The complete flowchart of the simulation algorithm is depicted in Fig. 5, whose steps are marked with curly brackets and described in the following subchapters.

2.5.1. Electricity control system

The simulation starts with the calculation of the nodal RE output {1} following (2).

$$P_{RE,\ n}(t) = P_{PV,spec,n}(t)^* P_{PV,rated,n} + P_{wind,spec,n}(t)^* P_{wind,rated,n} \quad (2)$$

The nodal electricity balance {2} is calculated by comparing the production $P_{RE,n}$ to the maximum possible electricity consumption of electrolysis and balance of plant (BOP) at each node. Based on the nodal electricity balance, a node can have either a local electricity surplus (when production is higher) or a local rated electricity demand. After the nodal balance, bilateral electricity contracts (BEC) {3} will be fulfilled. These BECs can be manually predefined, automatically set based on decision variables, or completely deactivated. The automated BECs are set in the pre-processing before the simulation by coupling all electrolysers to the closest node with sufficient RE installation. In the simulation step, BECs are fulfilled if the defined supplier has an electricity surplus and the recipient a rated electricity demand. After the PPAs, remaining surpluses and demands are processed by an algorithm representing a regional open electricity market (OEMA) {4}. Remaining rated demands are supplied from the remaining surplus, prioritising locations with the lowest hydrogen storage levels. After either all rated demands are fulfilled or no electricity surplus is left, the OEMA finishes. Remaining surpluses represent RE curtailment, which could be potentially sold to an external grid but will be ignored in the scope of this work. This decision arises from the fact that very high RE generation usually leads to very low electricity prices at the stock market. Remaining rated demands after the OEMA can, if allowed in the scenario, potentially be supplied by AES, in the scope of this work an acronym for hydropower, bioenergy, or external grid electricity. For the first two, plants need to be already installed at the location of the electrolysis. New installations of hydropower and bioenergy plants are not allowed in the system, as economically feasible potentials in Germany are already nearly used up. The AES is used if local hydrogen storages are low and/or the electricity price at the timestep is low. The conditions for use of the alternative electricity algorithm {5} are schematically depicted in Fig. 6. Hydropower, bioenergy, and external grid

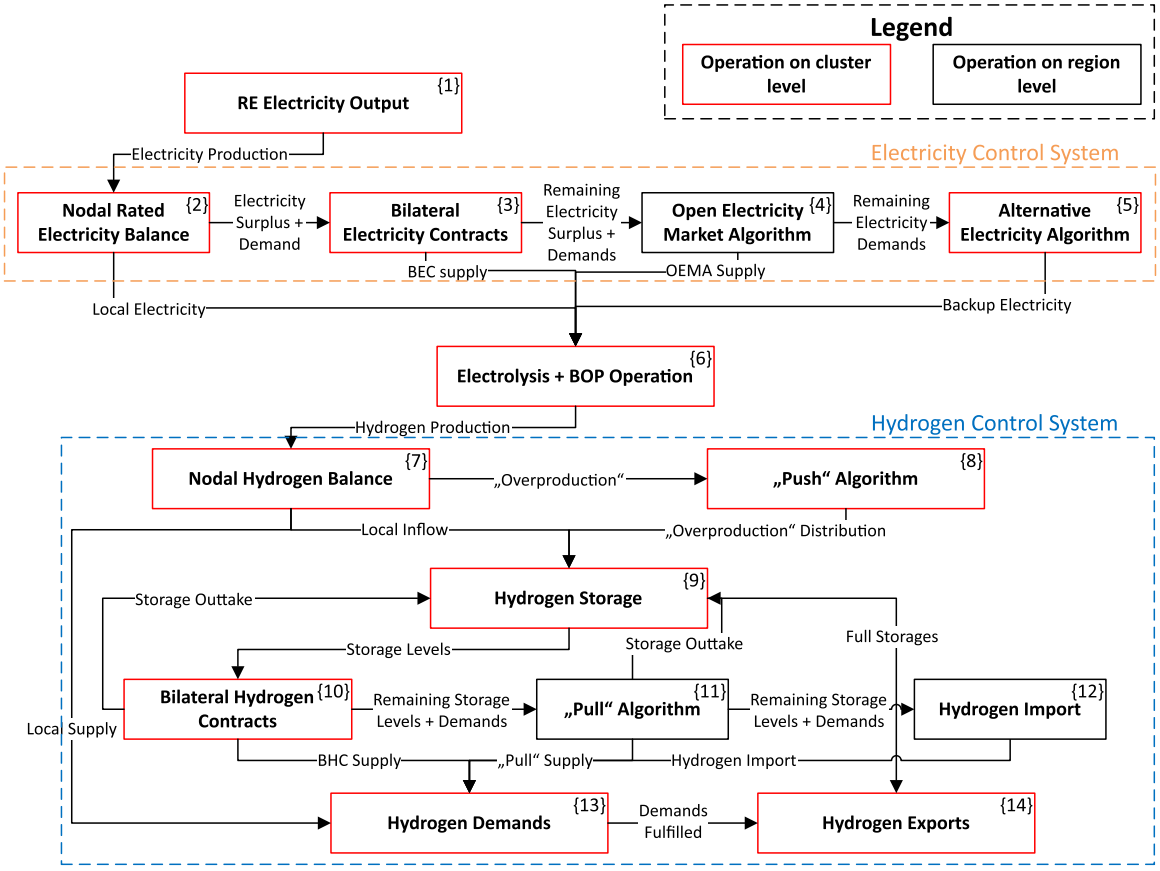

Fig. 5. Simplified flowchart of the simulation, which is performed at each simulation timestep in the Technical Model (as part of the model flowchart in Fig. 3). The RE production determines the electricity control system, which in turn determines the hydrogen production. Spatially resolved hydrogen production and demand define the hydrogen exchange.

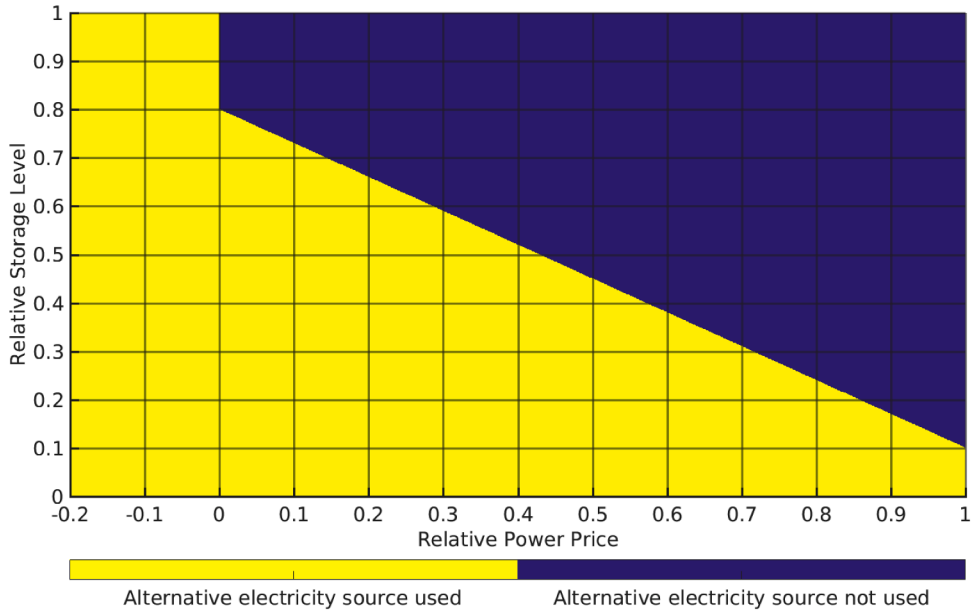

Fig. 6. Schematical depiction of usage of alternative electricity sources depending on storage level and power price. If prices and/or storage levels are low, electricity from alternative sources (hydropower, biomass, grid) is used if local RE is not sufficient.

electricity are treated similarly in the simulation with respect to local potentials, with the only exception that additional grid fees apply for external electricity and not for hydropower and bioenergy. This approach is taken based on the assumption that the operator of the electrolysis has to pay the same electricity price as hydropower or bioenergy would achieve at the electricity stock market.

After all steps of the electricity algorithm, the electricity flows are aggregated at each node and passed to the BOP and the electrolysis {6}, with the first having priority of supply. The electricity balance at each node n is depicted in (3) with h representing electricity source locations and i electricity-consuming locations. If a rated demand of the electrolysis cannot be supplied, it is simply run at lower power or shut down. This approach assumes the flexibility of operation of low-temperature electrolysis and is not suited for high-temperature electrolysis. All flows of electricity are traced regarding power and energy for the economic calculation after the simulation.

$$P_{EL,\,n}(t) = P_{RE,n}(t) + P_{BEC,in,n}(t) - \sum_{i=1}^{n_{BEC,n}} P_{BEC,out,n,i}(t) + \sum_{h=1}^{n_{OEMA,in,}} P_{OEMA,in,n,h}(t) - \sum_{i=1}^{n_{OEMA,out,n}} P_{OEMA,out,n,i}(t) + P_{AES,n}(t) - P_{BOP,n}(t) \tag{3}$$

2.5.2. Hydrogen Control System

The hydrogen system starts with the electricity supply of the electrolysis. Details of the electrolysis operation can be found in Holst et al. [42]. The first step of the hydrogen control system is a local balance {7} between production and demand, resulting in net production or demand at each node. After the local balance, the remaining production is compressed and stored {9}. If hydrogen cannot be stored locally, the excess hydrogen can be transported to the closest storage with sufficient space left. This algorithm ensures maximum usage of hydrogen and will be labelled as "push transport" {8}. It can be deactivated based on the scenario. Remaining demands that cannot be fulfilled locally are first supplied by bilateral hydrogen contracts (BHC) {10}. Similar to BECs, these connections can be manually defined, set automatically based on decision variables (demands are connected to the closest sufficiently large electrolysis), or deactivated. The BHCs are fulfilled if the supplier has sufficient hydrogen stored to fulfil the demand of the defined recipient. Remaining demand after the BHCs can be supplied from the open hydrogen market {11}, which is labelled as "Pull transport". This algorithm supplies demands with hydrogen transported from the closest node with sufficient storage content.

Several points need to be mentioned regarding the transport of hydrogen and the hydrogen exchange algorithms (HEA). First, the "push" and "pull" algorithms favour the transport of the complete surplus/demand to/from one location over splitting it in multiple amounts. Secondly, "closest location" does not refer to airline distance but to approximated transport costs for a standardised amount between locations to account for installed infrastructure and geographical aspects that can increase the transport costs substantially. Lastly, the transport is simulated as it would be done via pipeline, so hydrogen is transported in flexible amounts at any timestep and instantly. This is necessary because the economically optimal transport technology is not known before the simulation. A differentiation between transport technologies is only made after simulation in the economic system. The effects of this simplification are mitigated by ensuring that if trailer or rail transport is chosen for a specific link, sufficient storage capacity is installed automatically at both the origin and destination of the transport link.

An additional supply component of the hydrogen system is the import of hydrogen {12} from outside the region. This can be activated or deactivated based on the respective scenario and is possible at locations with import capabilities and infrastructure like a connection point to the hydrogen backbone. To allow import of hydrogen, an import price needs to be defined. In the simulation, imported hydrogen is used whenever hydrogen demands cannot be fulfilled within the region (insufficient production and empty storages). Similar to hydrogen import in times of empty storages, the export of hydrogen {13} produced from local RE in times of full storages can be activated. To allow hydrogen export, an export price needs to be defined, which will be used to calculate the economic benefits from exporting hydrogen. Depending on the export price and RE potentials, this might create an incentive for the optimisation algorithm to install larger facilities than needed for local hydrogen demands. Import and export of hydrogen can occur at any time, based on the assumption that a national hydrogen backbone

has sufficient storage capabilities. The full hydrogen storage balance at each node n is displayed in (4), with i representing the locations of hydrogen production and j the locations of hydrogen consumption.

$$m_{stor,\ n}(t) = m_{EL,\ n}(t) + m_{BHC,in,\ n}(t) - \sum_{j=1}^{n_{BHC,n}} m_{BHC,out,n,j}(t) + \sum_{i=1}^{n_{Push,n}} m_{push,n,i}(t) - \sum_{j=1}^{n_{pull,n}} m_{pull,out,n,j}(t) + m_{Import,\ n}(t) - m_{Export,\ n}(t) - m_{con,\ n}(t) \quad (4)$$

2.6. Economic Evaluation

The economic evaluation calculates economic and technical KPIs based on the decision variables and simulation results. The most important result and objective of the optimisation in the scope of this work are the total system *LCOH*, which are the sum of the $LCOH_q$ for each cost component q (5) calculated with the annuity method according to (6). The capital recovery factor CRF_q is based on the component lifetimes $t_{life,q}$ and the weighted average cost of capital (WACC) according to (7).

$$LCOH = \sum_{q=1}^{Q} LCOH_q \quad (5)$$

$$LCOH_q = \frac{CRF_q * Capex_q + Opex_q}{m_{H2,total,prod}} \quad (6)$$

$$CRF_q = \frac{(1+WACC)^{t_{life,q}} * WACC}{(1+WACC)^{t_{life,q}} - 1} \quad (7)$$

Capital expenditures (CAPEX) of facilities are calculated by multiplying a size variable, directly or indirectly based on decision variables, with constant specific costs or a cost function if economies of scale apply. The latter is the case for electrolysis, hydrogen storage, and hydrogen compressors. Exact values and functions, as well as a full list of all cost components, can be found in the supplementary material. Numerous cost functions, e.g., for electrolysis and hydrogen compressors and storages, are implemented with economies of scale enabled from the nonlinear modelling setup. The costs for hydrogen transport technologies, which are the special focus of this work, are explained in the following.

2.6.1. Transport Between Clusters

Transport between clusters labelled as between-cluster transport (BCT) is possible via road, pipeline, or rail networks. The total transported amount, or transport capacity, is not limited for any transport link, as it is assumed sufficient transport infrastructure will be implemented if necessary. The total depreciated costs for each possible transport mode are calculated for all active transport connections between two locations. For each connection, the transport technology with the lowest costs is selected. Therefore, only costs for one transport mode per connection are added to the total system costs.

Costs for road-based transport depend on travel distance and time (provided by the *Openrouteservice* [52]), the total transported amount between the locations, and the maximum hydrogen transported in one day in the whole region. This implies that trucks and trailers can be shared within the region by a region-wide operator of hydrogen transport. Based on this, the number of trucks in the whole region and the share of each connection at the total transported mass is calculated to get the costs for trucks, trailers, filling stations, and drivers. Economic details are given in the supplementary material. Integer truck numbers and degressive costs for filling stations are implemented. Transport by truck trailer is possible between all clusters.

Much higher amounts can be transported in one delivery over rail compared to road transport, as multiple railcars can be connected in one train. The railcars are operated in trailer switch mode and therefore function as mobile storages. This way, the train needs to operate less frequently as one railcar always remains at the destination until it is completely emptied. The downsides of rail transport are long driving times and high costs for use of the rail network. Technical and economical parameters for rail transport can be found in the supplementary material and are mainly taken from [53]. Transport per railcar is possible between any two clusters that are connected by the existing railroad system.

Pipeline-based transport is implemented as point-to-point transport only. A pipeline network connecting multiple locations, as presented by Forghani et al. [31], is under consideration for future versions of the model but would require a substantial change in the functionality of the HEA. For each point-to-point transport, the pipeline diameter is determined with the Panhandle equation for hydrogen taken from [54]. Based on the maximum mass flow determined by the region simulation, a desired output pressure at the end of the pipe, and a maximum flow speed [55], the equation is solved iteratively with increasing pipeline diameter until the necessary input pressure does not exceed maximum pipeline pressure. This implies that no recompression is needed, which is an acceptable assumption for the regional scope of this work. CAPEX and operational expenditures (OPEX) for pipe and compressor are calculated with respect to the pipe diameter and length and compression needed. Parameters and cost functions for the pipeline calculation can be found in the supplementary material. Both technical and economic equations for pipeline transport are implemented in high detail, benefitting from the nonlinear framework. Pipeline-based transport can be realised by means of new pipes or retrofitting of existing grids. The first can be installed between all clusters in the scope of this work. Pipeline retrofitting is implemented in the model, but there is no publicly available data on distribution networks, only transmission lines. As these are much larger and are of great importance for the national gas grid, a retrofitting within the regional scope is both not economically viable and questionable. Therefore, it is not present in the scope of this work.

Transport of hydrogen to and from import/export locations (if allowed in a scenario) is calculated similarly to BCT between each cluster centroid and its closest import location. The transport costs are calculated for each transport mode, and the cheapest costs are added to the system cost. If road transport is chosen, the trucks and trailers are shared in a pool together with the BCT.

2.6.2. Intracluster Transport

Although the spatial resolution of the system is bound to the cluster level and hydrogen applications within one cluster cannot be differentiated, costs for intracluster transport (ICT) of hydrogen are included if a cluster has two or more demand locations. Costs are calculated for transporting the total demand within the cluster $m_{dem,n}$ divided by the number of locations $n_{dem,n}$ over the mean distance between the cluster centre and demand location $\bar{d}_{trans,IC}$ and then multiplied by the number of demands as shown in (8). ICT can be done via trailer or distribution pipeline grids. Similar to BCT, only the cheaper mode is selected for each cluster. A combination of both ICT modes within one cluster is not possible, as the model cannot differentiate below cluster level.

$$C_{trans,IC,n} = costfcn_{trans,IC}\left(\frac{m_{dem,n}}{n_{dem,n}}, \bar{d}_{trans,IC}\right) * n_{dem,n} \quad (8)$$

2.7. Comparison of the Proposed Methodology to Existing Models

This section undertakes a qualitative comparison of the functionality of HYSCOPE with other modelling approaches presented in the literature and listed in Appendix Table 1 and Appendix Table 2. A quantitative comparison is not possible because the modelling approaches and their case studies are not open-source.

HYSCOPE is distinguished by its status as the first nonlinear model to incorporate a dynamic simulation of a spatially resolved HSC.

Additionally, it is noteworthy for its pioneering use of spatial clustering to define spatial resolution in a techno-economic optimisation model, a technique that prior to this, had only been applied in the context of energy system analysis [12,56].The technical scope of HYSCOPE is notably broad, encompassing a diverse range of electricity sources, including PV, WPP, hydropower, bioenergy, and grid electricity, in addition to multiple hydrogen application sectors. The only other model found in literature comparing truck trailer, railway, and pipeline transport is a static modelling approach by Parker et al. [28].

One disadvantage of HYSCOPE is that operation must be defined through a simulation heuristic. Operational decision variables, as used by He et al. [37] and Wang et al. [38], are not solvable in nonlinear optimisation, which may lead to nonoptimal operation strategies. Furthermore, the technical representation of hydrogen transport technologies is limited. The current form of HYSCOPE does not implement a pipeline network connecting multiple locations (see Forghani et al. [31]) or the timely-resolved representation of truck operation and mobile storage capacities (see He et al. [37]), in an effort to reduce modelling complexity. Furthermore, HYSCOPE is devoid of an ecological analysis, akin to the one presented by Genovese et al. [40], and relies exclusively on electrolysis for hydrogen production, disregarding alternative production technologies such as steam methane reforming or biomass gasification.

2.8. Case Study

2.8.1. Study Region

The developed and presented methodology of HYSCOPE is demonstrated on the SURR, which has already been studied as part of the project "Wasserstofftechnologien am südlichen Oberrhein – H2SO" [57]. The outline of the SURR and its most important geographic characteristics for this analysis can be seen in Fig. 7. The hydrogen demands, visible as red dots, are located at industrial sites based on research of multiple sources (potential industrial hydrogen consumers [58], current hydrogen applications [59], current industries from waste heat [60] and pollution register [61], chemical industry parks [62], and locations provided by the *German Hydrogen Association (DWV)* in project "PowerD" [63]). These locations get combined with demand projections developed within the project of which the presented work is part of; details can be found in [64]. Within the project, defossilisation pathways for the European industry sectors have been developed, and the resulting hydrogen demands have been quantified per NUTS 3 region [65]. For the regional analysis of this work, the hydrogen demands are distributed per sector among existing industrial locations to achieve the required spatial resolution. Additionally, a network of to-be-built hydrogen refuelling stations is pre-optimised to supply all expected hydrogen mobility demands, surveyed in the *H2SO* project, within the region with minimal investment and operation cost. The methodology of

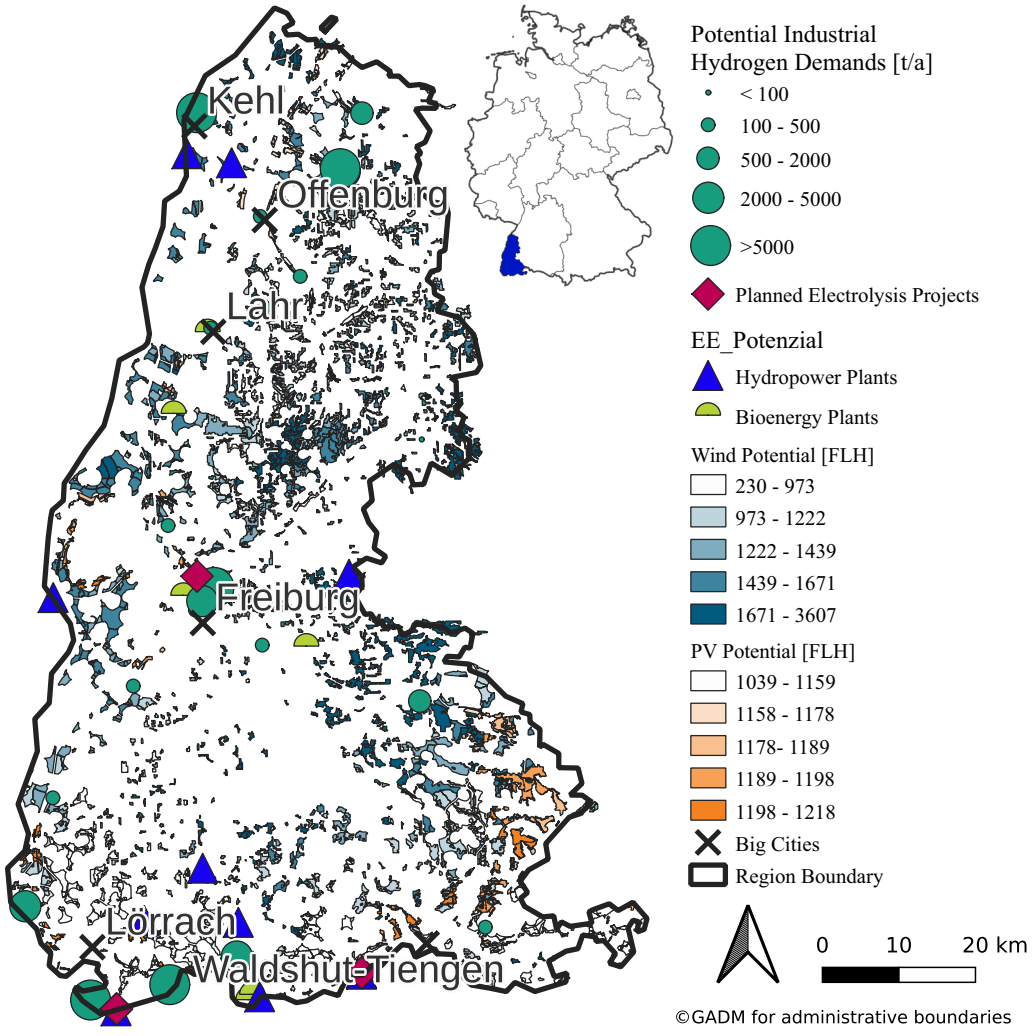

Fig. 7. Most relevant geographic features of the SURR. Potential areas for RE form the main electricity sources that can be complemented by hydropower or biomass. The displayed hydrogen demands need to be supplied by the optimised hydrogen supply chain.

this can be seen in [66].

Besides potential hydrogen applications, the most important geodata for hydrogen valleys are the locations of existing and potential RE plants. Suitable areas for the installation of PV or WPP are based on the *Agora Photovoltaic- and Wind Area Calculator,* which shows potential areas in Germany in terms of land use and distance restrictions [67]. A minimum distance of 600 m was set as restriction, and existing RE plants were subtracted from the theoretical potential areas. Only contiguous areas with a minimum potential of 1 MW installed capacity were considered. In addition to PV and WPP, the main sources of future green electricity, hydropower and bioenergy could be important sources to increase the electrolyser full load hours (FLH) during the build-up of the hydrogen system. As the potential of sufficiently large plants is already highly exploited, the use of existing plants is more realistic. Therefore, existing plants are taken from the German *Market Master Data Register* [68]. As for PV and WPP, only plants with a minimum rated capacity of 1 MW were considered.

2.8.2. Modelling scenarios

Table 1 lists all scenarios analysed in the scope of this work. They are grouped and marked with a colour by four main questions that each group shall analyse:

I) What is the impact of the spatial resolution in modelling (green)?
II) What effect has a change to spatially constrained hierarchical clustering that performed nearly as good as REDCAP in [44] (yellow)?
III) What role do the hydrogen exchange algorithms play (see section Hydrogen Control System) (red)?
IV) How do the optimal infrastructure changes when import and export of electricity or hydrogen is possible (blue)?

2.8.3. Computational details

The optimisations were performed on *bwUniCluster 2.0*, a high-performance cluster of the universities of Baden-Württemberg. Each run is calculated on a node with an Intel Xeon Gold 6230 with 64 cores, a frequency of 2.1 GHz, and a total RAM of 180 GB.

Different stopping criteria were used. In the best case, CMA-ES is stopping on a stall of the objective function value (the LCOH), which is defined in a scope of this work as a relative improvement smaller than 10^{-5} in the last 100 generations of CMA-ES. This triggers a new optimisation with a new random starting population. An optimisation is also terminated after 1000 generations if no objective function stall was reached. Ten total optimisation runs are started, and the lowest minimum of all is the final result that is displayed in figures and tables of the result section. In scenario group I, the result spread of all ten optimisation runs is analysed. As single jobs on the bwUniCluster 2.0 are limited by three days of total computation time, this limits the actual number of optimisations within one job for scenarios with a higher number of clusters. For scenarios with a higher cluster number in the spatial resolution comparison, multiple jobs need to be calculated. This is a severe disadvantage regarding their practicability.

3. Results and discussion

3.1. Spatial resolution comparison

This group of scenarios is used to analyse the impact of the spatial resolution, in other words, the number of subregions, on the optimisation results. Each subregion is represented as one node in the model. A coarse resolution usually has higher aggregation errors, as all points of interest need to be treated as being at one location, and averages need to be used for differences within the subregion. On the other hand, a finer resolution has higher computational efforts and a higher risk that the nonlinear optimisation algorithm provides only a local optimum that is substantially worse than the global optimum. Therefore, a good trade-off needs to be found.

The false aggregation in large subregions of a coarse resolution can have several effects on the results. Most of them lead to an *underestimation* of cost, which includes the following:

- There is no intracluster electricity transmission cost because of the assumption that electricity that is used in the same cluster as it is generated is used “on-site”. Therefore, multiple electricity generation facilities (PV, WPP, hydropower, and bioenergy) are treated as being at one location. Naturally, this error gets more substantial with larger cluster size.
- Economies of scale are included for various technologies of the HSC (electrolysis, H2 storage, pipelines). This might be overestimated in very large clusters, in which the value of one node might represent multiple facilities.
- Similarly, there are fewer BCT connections in a coarse resolution that additionally benefit from economies of scale (larger pipelines, higher utilisation of trucks). This is partly balanced by ICT.

On the other hand, there are effects from aggregation that might lead to an *overestimation* of cost, including the following:

- An average of the possible locations for PV and WPP installations is used to calculate the specific production timeseries. On finer cluster resolution, very good RE locations might be better represented and can be specifically used by the optimisation.
- With increasing cluster number, more hydrogen demands are represented by single clusters in which no ICT occurs. This might be more realistic, as these large demands would be addressed directly instead of transporting to a cluster centre first before distribution.

The significance of each effect shall be evaluated based on the modelling results. Additionally, simulation and optimisation time and performance will be analysed.

Fig. 8 depicts the LCOH per cost component for optimisation with increasing spatial resolution, while Table 2 shows selected results. The results for all KPIs can be found in the supplementary material. As expected, more hydropower and less PV plants and WPP are utilised in coarse resolutions, which also leads to less H2 storage demand. ICT is only relevant up to 20 clusters. Contrary to initial expectations, the BCT has no clear trend. Instead, electricity transport is increasing with cluster number and accounts for the larger share of energy exchange. This is displayed with the ratio for the transported amount of electricity $r_{elec,trans}$ and hydrogen $r_{H2,trans}$ compared to the total amount (which also includes the hydrogen and electricity used on-site). While the ratio has no clear trend for hydrogen, it continuously grows for electricity. Comparing the total LCOH, a maximum can be seen for 20 clusters. For this spatial resolution, the expenses for the transport of electricity and hydrogen are already high, but the average FLH for RE is still substantially lower than for finer spatial resolutions. Looking at more results from Fig. 8, the number of electrolysers stays relatively constant from 20 to 80 clusters. The optimisation does not install more electrolysers in smaller clusters to benefit from economies of scale. Therefore, around ten electrolysers are sufficient for supplying the whole region.

Simulation time grows substantially with higher cluster numbers. Because of this and a more complex optimisation, ten iterative optimisations can only be completed in 72 hours for a spatial resolution of up to 20 clusters. Four runs could be finished for *CL40*, while only one or two were possible for a finer resolution. Multiple computation jobs were necessary to reach ten optimisation runs. Interestingly, the spread between the best and worst optimisation, displayed in red in Fig. 8, is relatively constant even with increasing spatial resolution and therefore optimisation complexity (besides the very coarse resolution *CL5*). Nevertheless, *CL40* proved the most stable optimisation results and therefore will be used as the spatial resolution for the scenario groups C and D. This also guarantees at least four completed optimisation runs

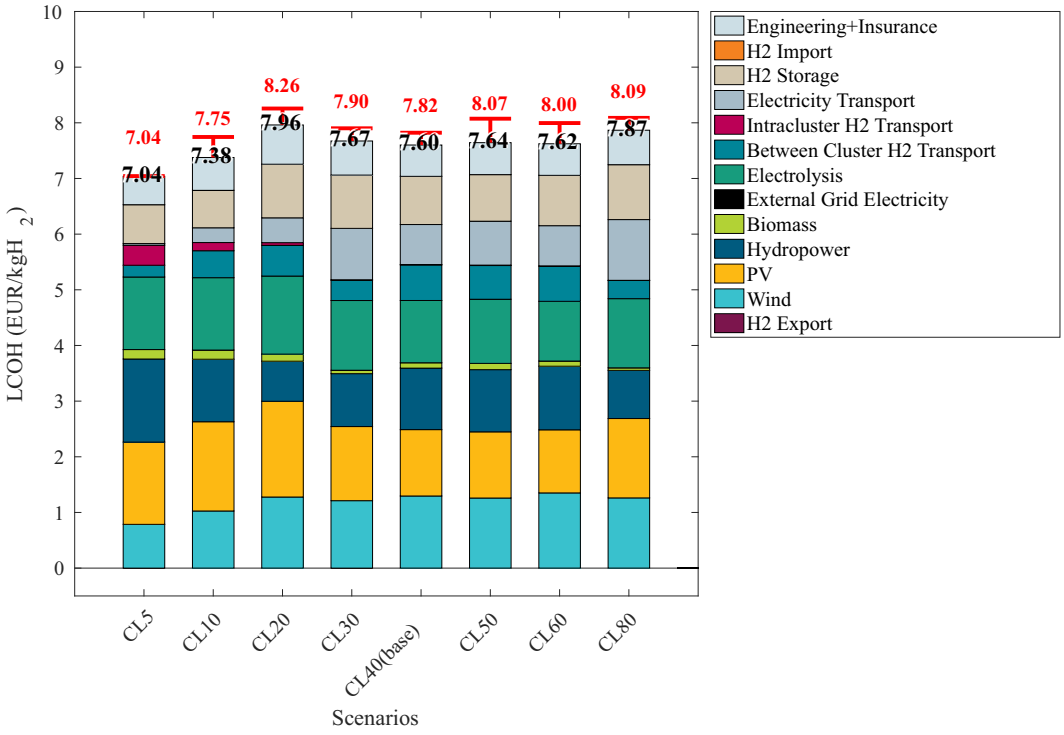

Fig. 8. Component-wise LCOH for scenario group I. The composition is shown for the best optimisation, and the spread and maximum of the optimisation runs are displayed in red. The main differences are the intracluster transport cost (high for low resolution, i.e. large clusters) and the between-cluster transport cost (high for high resolution, i.e., many clusters).

Table 3
Selected results for scenario group II. The differences between spatial resolution produced from the same spatial algorithm are larger for SCHC than for REDCAP.

Result	Unit	CL20 (REDCAP)	CL40 (REDCAP)	CL80 (REDCAP)	CL20 (SCHC)	CL40 (SCHC)	CL80 (SCHC)
LCOH	€/kg	7.96	7.60	7.86	7.50	7.74	8.19
$FLH_{WPP,mean}$	h	2070	2408	2330	2520	2495	2311
$m_{Truck,total}$	t	20,604	22,732	17,803	10,446	11,929	38,897
$m_{Pipeline,total}$	t	28,252	20,928	14,072	46,926	24,635	1921
$m_{Rail,total}$	t	0	0	0	1250	0	0

within reasonable computation time.

3.2. Spatial clustering algorithm comparison

In the second scenario group, the optimisation results of three clustering runs with SCHC are analysed and compared to the results based on clustering with REDCAP for the same number of clusters (*CL20, CL40* and *CL80*). Both clustering algorithms performed similarly well in [44].

Table 3 lists selected results for the scenarios of group II. In general, both spatial clustering algorithms were similarly well suited for the optimisation; therefore, only the KPIs with the biggest difference are shown. It is apparent that the differences between the coarse and fine spatial resolutions of SCHC are substantially larger than the coarse and fine spatial resolutions clustered with REDCAP. Especially the LCOH for *CL20_SCHC* are more than 0.7 €/kg_{H2} lower than for *CL80_SCHC*, which is mainly based on the better selection of good WPP locations and therefore substantially higher FLH of WPP. While SCHC performed better in allocating good WPP sites in 20 clusters, the differences between coarse and fine resolution, especially regarding the transport infrastructure, might indicate that *CL20_SCHC* is not a good representation of the region. The high share of pipeline transport and the use of rail transport were not apparent in any other scenario optimised. Nevertheless, despite these differences, the visualisation of *CL20_REDCAP* and *CL20_SCHC* in Fig. 9 shows a similar hydrogen system with only one large electrolyser being at a different location. This confirms the conclusion that both spatial clustering algorithms are suitable for the optimisation with only small differences, like the better allocation of WPP areas for small clusters with SCHC. Nevertheless, the difference between the spatial resolutions of REDCAP was smaller than the ones of SCHC; therefore, this is seen as slightly more stable spatial clustering.

3.3. Hydrogen exchange algorithm comparison

This group of scenarios is compared to analyse the relevance of the hydrogen exchange algorithms presented in Section 2.5.2. The algorithms BHC, Push, and Pull, which are all activated in the base scenario, are tested in all possible combinations. An optimisation with Push only is not performed, as demands would not trigger transport and are therefore unfulfilled, which leads to penalties.

Fig. 10 shows the share of cost components in the LCOH for the optimisations with different HEAs activated on the resolution of *CL40*. All scenarios have higher LCOH than the *base* case with all HEAs activated. Especially the optimisation for *BHC* is substantially more expensive, as each demand can only be fulfilled on-site or from one pre-

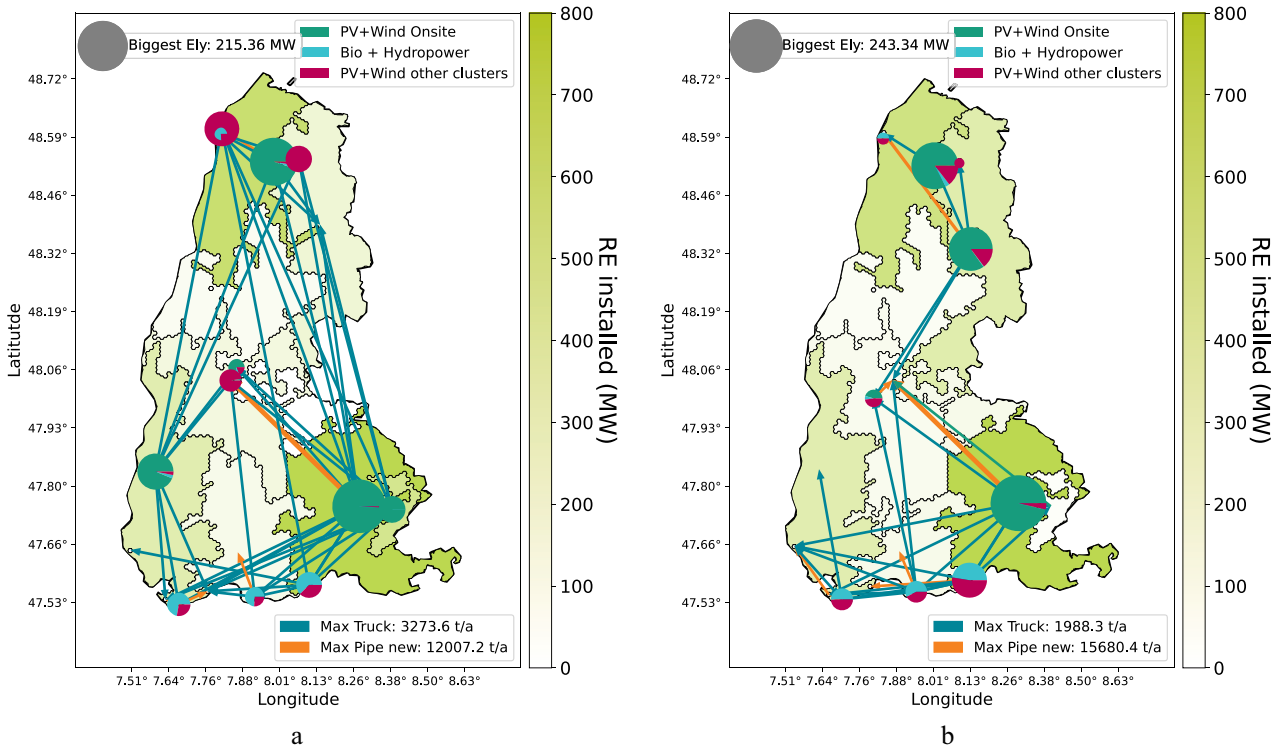

Fig. 9. RE installations (background colour), electrolyser locations and supply (circles), and hydrogen transport links (arrows) in 20 subregions clustered with REDCAP (a) and SCHC (b). Similar subregions from clustering result in similar optimisation results.

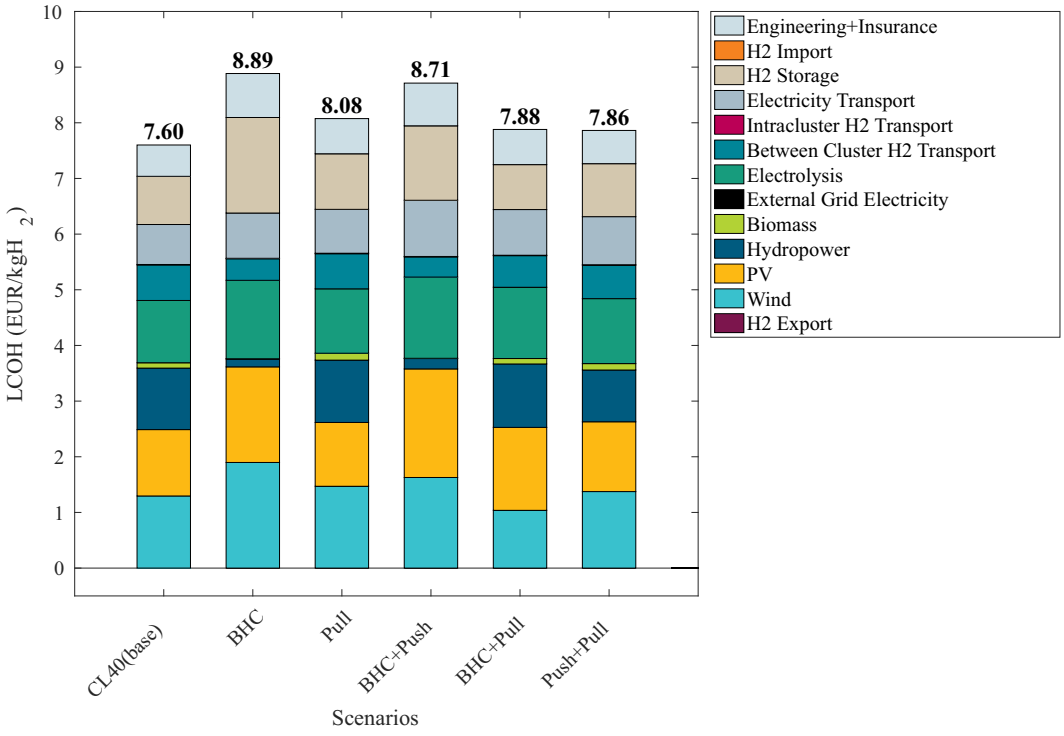

Fig. 10. Component-wise LCOH for scenario group III. Scenarios without the Pull algorithm have substantially lower use of hydropower but higher costs for RE and hydrogen storage. A combination of all exchange algorithms leads to the lowest cost.

Table 4
Selected results for scenario group III. Push algorithm helps to avoid H2 loss because of full storages. Demand supply via the Pull algorithm proves to be most important for low LCOH.

Result	Unit	CL40 (base)	BHC	Pull	BHC+Push	BHC+Pull	Push+Pull
LCOH	€/kg	7.60	8.89	8.08	8.71	7.88	7.86
$m_{H2,prod}$	t	62,455	64,899	65,183	62,215	65,037	62,171
$m_{H2,loss}$	t	0	2314	3248	0	3085	0
# transport links	-	77	17	67	28	47	86
Transport performance	t*km	2,295,779	3,481,807	3,589,332	1,976,623	3,509,411	2,256,116

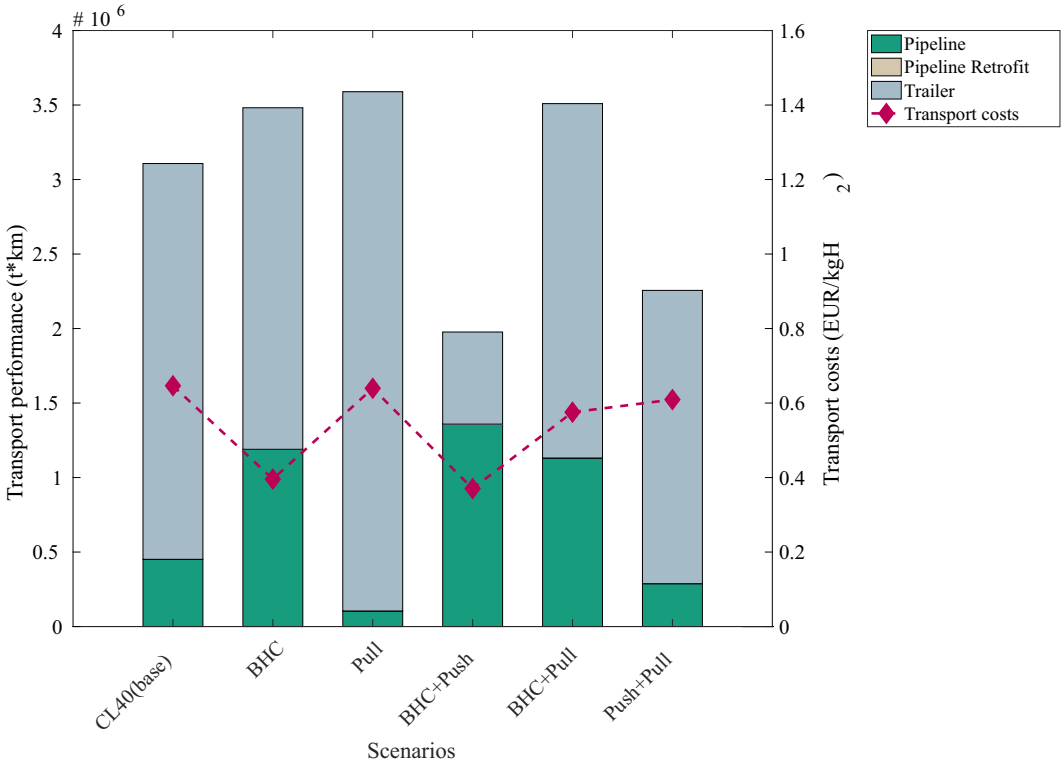

Fig. 11. Transport performance and specific transport cost for scenario group III. The low specific transport costs for scenarios without Pull transport are negated through larger transport volumes and generally higher costs. No pipeline retrofit is used, as only data for the natural gas transmission grid with large diameters was available.

defined transport connection. Therefore, the system cannot react to local shortages or overproduction of demands, which especially leads to higher storage costs. Especially reacting to demand shortages with the Pull algorithm is important and reduces costs substantially because of lower demands for H2 storages and electrolysis overdimensioning. The detailed results in Table 4 show that in scenarios without Push exchange, some hydrogen is not storable because of full storages (up to 5 % of total production). The activation of BHCs leads to a reduction in transport links between locations but an increase in transport performance, visualised in Fig. 11. This also leads to more use of pipeline transport, as this benefits from economies of scale due to the smaller number of transport links. The specific transport costs in scenario *BHC* are substantially lower, which illustrates that the highest total cost of this scenario comes from other components, especially RE and H2 storage. Fig. 12 visualises spatially resolved results for scenario *base* and *BHC*. It illustrates that the number of transport links is smaller in *BHC*, but the links are substantially longer and have a higher transported mass on average. The difference in algorithms does not only affect the transport links but the whole setup, resulting in a substantially larger electrolyser in scenario *BHC* and different electrolyser positions.

The comparison within scenario group III demonstrates the benefit of each HEA. BHCs lead to a centralisation and economies of scale in pipeline transport. Push prevents hydrogen loss on overproduction and Pull offers flexible demand supply. Therefore, a full combination of all HEAs is recommended, although the design of contracts might be more complicated in reality with various market participants and stakeholders' interests. Transferred to reality, that means that the currently dominating approach of bilateral contracts might lead to overall higher costs and that an approach including intermediary gas transport/trading companies might lead to lower costs.

3.4. Import option comparison

The fourth scenario group is assessed to evaluate the influence of import and export options of electricity and hydrogen on the optimisation results. As future prices for buying and selling electricity or hydrogen are highly speculative, the focus of the comparison is less on absolute values but more on a change of functionality. In the scope of this work, an average electricity price of 97.24 €/MWh (average German stock market price of 2021 [46]) and an assumed hydrogen import price of 7 €/kg_{H2} and export revenue of 6 €/kg_{H2} will be used. This is in line with current hydrogen price projections [69] and results from the

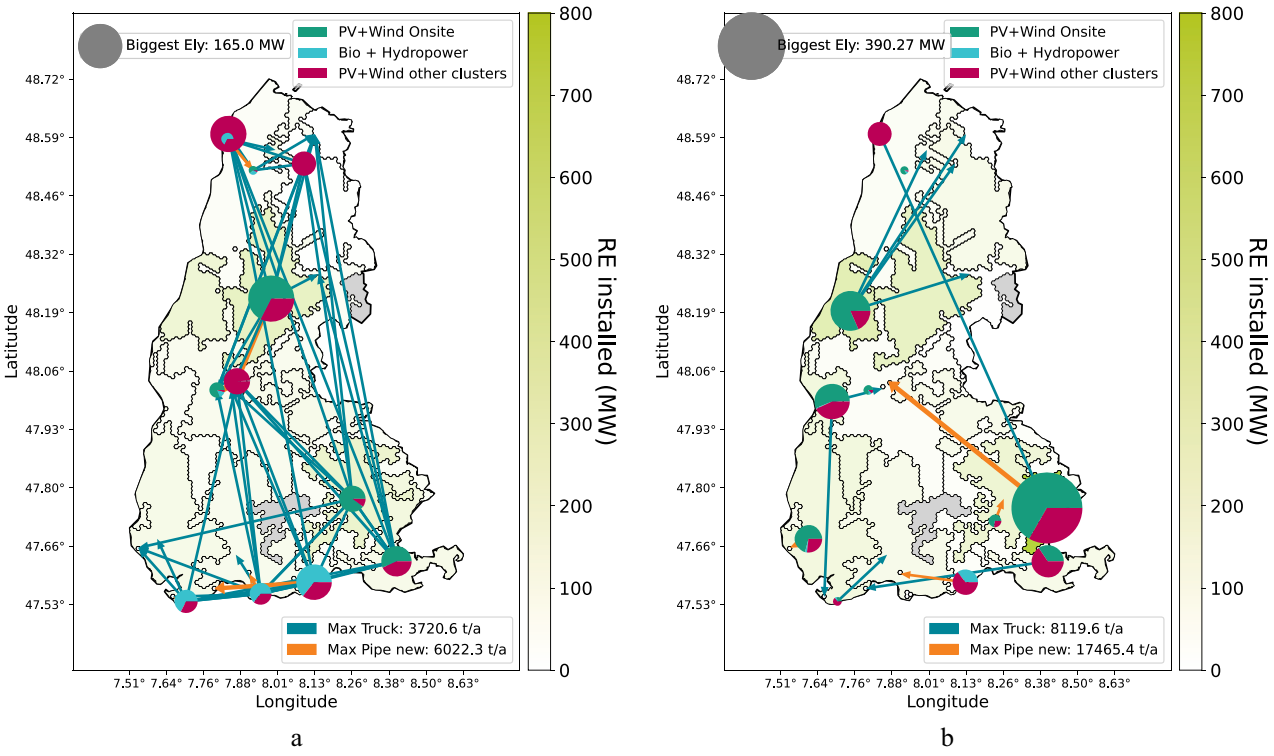

Fig. 12. RE installations, electrolyser locations and supply, and hydrogen transports in scenario base (a) and BHC (b). Hydrogen exchange by BHC only leads to a substantial centralisation of electrolysis and transport, but the economies of supply cannot compensate for the low flexibility of the exchange algorithm.

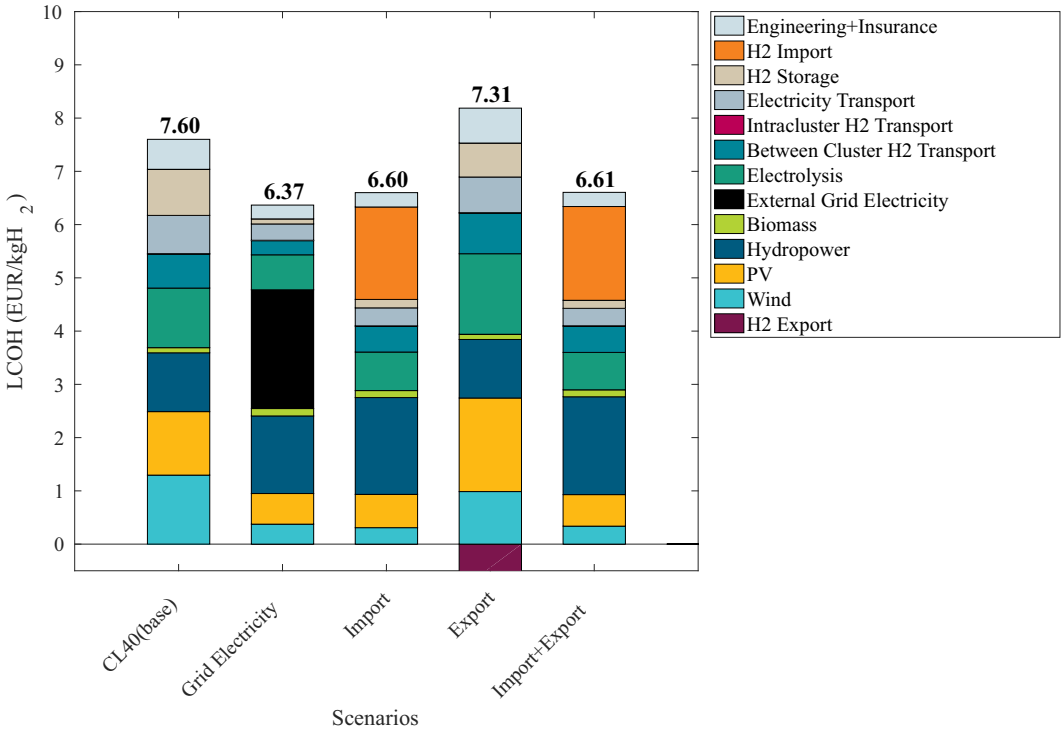

Fig. 13. Component-wise LCOH for scenario group IV. The addition of grid electricity or hydrogen import substantially lowers LCOH within the region, due to below-average local RE potentials. Export can reduce some costs, as it offers flexible revenues in times of high production.

Table 5
Selected results for scenario group IV. The setup of the optimised supply chain is strongly influenced by the change in boundary conditions. Especially the storage hydrogen demands decrease from the flexibility of electricity and hydrogen imports.

Result	Unit	CL40 (base)	Grid Electricity	Import	Export	Import+Export
LCOH	€/kg	7.60	6.37	6.60	7.31	6.61
$P_{PV,total}$	MW	1354	653	710	1995	673
$P_{Wind,total}$	MW	516	150	123	393	135
$P_{Ely,total}$	MW	681	373	435	934	419
$V_{storage,H2,total}$	m^3	191,742	10,735	8896	106,201	8388
$E_{RE,total}$	GWh	2850	1179	1210	3335	1186
$E_{Grid,total}$	GWh	0	1055	0	0	0
FLH_{EL}	h	4589	8299	5379	3839	5556

project “TransHyDE-Systemanalyse”.

Fig. 13 depicts the LCOH for the import scenarios. Importing electricity or hydrogen for these prices offers a substantial cost decrease for SURR. Although imported hydrogen makes up only about one-fifth of total demands, the flexibility of import at any time helps to gap production lows and reduces H2 storage demands substantially. This leads to a total reduction of LCOH by around 15 %. Exporting hydrogen for 6 €/kg is not very attractive for the production conditions in SURR, but it will still be used as a flexibility option. A larger dimensioning of production facilities helps to fulfil demands, as overproduction can be sold for revenue at any time. If import and export are possible, export is not used, as import already offers flexibility; therefore, the results of this scenario are nearly identical to import only. Table 5 lists selected detailed results that especially demonstrate the differences in H2 storage size, the sizing of RE and electrolysis, and the FLH of electrolysis, which are nearly doubled by the option for importing grid electricity.

3.5. Comparison to hydrogen strategies worldwide

Despite the utilisation of a German case study in this work, HYSCOPE is not confined to specific world regions and can be applied globally if the necessary local input data is available. This section explores the relevance of the proposed modelling framework and the results derived from it for hydrogen valley projects and hydrogen strategies published by countries worldwide. The Clean Hydrogen Partnership which is funded by the European Union, has identified four characteristics that define a hydrogen valley: large in scale, high value chain coverage, supply of more than one sector, and a geographically defined scope [70]. Similar characteristics have been defined by the United States [71]. All of these characteristics are covered within HYSCOPE and apply to the case study SURR. The total demand assumed for the region of 62 kt/a is substantially larger than the minimal 4 kt/a necessary for a large-scale hydrogen valley [70], because demand projections for the 2030 s were used. A further publication focussing on early stages and possible transformation pathways analysed with HYSCOPE is currently under development.

The prospect of nuclear power generation has been a subject of consideration within certain hydrogen valleys in the United States. While not directly implemented in HYSCOPE, the construction of new dedicated plants for hydrogen production is deemed unfeasible; therefore, the representation would closely mirror that of renewable baseload or grid electricity demonstrated within the case study SURR. The strategy of the United States [71] further mentions the use of hydrogen for backup electricity, but this would require the implementation of further electricity demands or the combination with an energy system analysis. HYSCOPE does not incorporate less-likely hydrogen applications, such as the injection into the natural gas grid [6] or residential heating [71], as many European strategies argue against them [7,9]. The European hydrogen strategies, including the German [7], Dutch [10] and Spanish [9] strategies, emphasise the long-term integration of the hydrogen valleys into the European Backbone as a crucial aspect. Contrary to the majority of other model-based studies on hydrogen valleys, HYSCOPE and the present study analyse the influence of hydrogen imports and exports via the backbone (see Section 3.4). The analysis reveals that cooperation among local stakeholders and the sharing of infrastructure are identified as key advantages of hydrogen valleys across all the analysed hydrogen strategies. This assertion is substantiated by the cost benefits of flexible hydrogen supply algorithms presented in Section 3.3. A methodology for facilitating stakeholder collaboration is the "H2 Matchmaker", a software currently under development for the United States [72]. A combination with HYSCOPE appears advantageous. The significance of hydrogen valleys as export hubs is a particular focus in non-European strategies. Consequently, the enhancement of HYSCOPE with respect to ship-based export of hydrogen and sustainable fuels is under consideration. The potential benefits of this approach are evident in the potential for local hydrogen consumers within the exporting nation to be connected with the production site, a process for which HYSCOPE has the capacity to generate valuable results.

4. Conclusion

This work demonstrates the methodology and potential of a spatially resolved, dynamic optimisation of regional hydrogen supply chains. The framework combines the strength of multiple approaches: dynamic simulation for time-dependent operations (e.g., fluctuating electricity production), spatial resolution for optimisation of plant locations and necessary transport technologies and nonlinearity for realistic technical and economic equations. The functionality of the model framework has been demonstrated on a representative region in Southern Germany but could be applied in hydrogen regions worldwide if sufficient high-quality input data is available.

The impact of four groups of modelling scenarios was analysed, quantified, and discussed, each set to answer different leading questions regarding modelling performance. Optimisation with different spatial resolutions showed that a very coarse resolution leads to an underestimation of cost due to false aggregation and underestimated exchange cost, but simultaneously showed a cost decrease after a maximum due to better representation of good renewable electricity sites and hydrogen applications. The base case for an autarkic region operation resulted in average hydrogen supply costs of 7.60 €/kg, half of which consist of electricity costs evenly spread between photovoltaics, wind power, and hydropower. Optimisations with only bilateral hydrogen supply contracts result in 15 % higher cost. On the other hand, the addition of grid electricity reduced cost by 1.25 €/kg, and the option for hydrogen import reduced cost by 1 €/kg.

The modelling framework demonstrated that it could help to answer questions stated at the end of the introduction section. The questions regarding centralisation and optimal transport technologies depend on location and scenario. If only bilateral hydrogen supply contracts are used, a stronger centralised system with larger electrolysis and a higher share of pipeline transport results from optimisation. In most scenarios, a balanced mix of electricity sources was utilised, enabling 3500 to 5000 full-load hours of the electrolysis. The break-even point for the hydrogen import price must be slightly below the assumed 7 €/kg based on the share of one fourth of imported hydrogen of the total demand in the respective scenario.

The results presented in this work, as well as the methodology of the modelling framework. are subject to various limitations. Nonlinear optimisation algorithms are only capable of finding local optima. as demonstrated in the results of scenario group A. The effect of this is minimised through iterative optimisation of the same setup and the selection of the overall best optimisation result. The transport of hydrogen is represented in a simplified form in the simulation. This error is partly mitigated with additional storage costs for truck transport and minimum truck delivery numbers for each transport link. Technologies outside the model's system boundary that are only represented through exchange points could set further limitations. Although parts of the supply chain modelling, are validated with real data, a whole validation of the full system simulation is not possible, as no integrated hydrogen systems of this scale exist yet. Finally, like all modelling, the results depend on the quality of input data and parameters that have especially large ranges of uncertainties for future technologies and reference years.

Further improvements to the presented model framework can include realistic simulation of different transport technologies, Power-to-X synthesis as part of the hydrogen value chain, or algorithms to get location-specific levelized cost of hydrogen that are currently under development. Results will be shown in future publications. This also applies to results on other regions, helping to understand the specific suitability for hydrogen supply chains and proving the importance of the modelling. Furthermore, should the integration of the electrical systems be improved, e.g., by focusing more on the interaction with the national electricity grid or by implementing electrical energy storages. The allocation of results from the cluster level to exact locations will be considered for future work.

CRediT authorship contribution statement

Friedrich Mendler: Writing – original draft, Visualization, Software, Methodology, Formal analysis. **Christopher Voglstätter:** Writing – review & editing, Validation, Methodology. **Nikolas Müller:** Writing – review & editing, Visualization, Software. **Tom Smolinka:** Writing – review & editing, Supervision, Funding acquisition. **Marius Holst:** Writing – review & editing, Validation, Conceptualization. **Christopher Hebling:** Validation, Supervision. **Barbara Koch:** Validation, Supervision.

Declaration of competing interest

The authors declare that they have no known competing financial interests or personal relationships that could have appeared to influence the work reported in this paper.

Funding statement

This work was funded by the German Ministry of Education and Research (BMBF) within the research programme „TransHyDE-Sys - Systemanalyse zu Transportlösungen für grünen Wasserstoff" (funding reference number 03HY201K).

Computational support

This work was performed on the computational resource bwUniCluster funded by the Ministry of Science, Research and the Arts Baden-Württemberg and the Universities of the State of Baden-Württemberg, Germany, within the framework program bwHPC.

Data availability statement

Detailed optimisation results can be found in the supplementary materials. Further data will be made available on request.

Ethical standards

The research meets all ethical guidelines, including adherence to the legal requirements of the study country.

Supplementary materials

Supplementary material associated with this article can be found, in the online version, at doi:10.1016/j.adapen.2025.100207.

Appendix A: List of related previous modelling activities

Tables A1 and A2.

Appendix Table 1
Relevant previous studies in which static optimisation models for hydrogen supply chains have been applied.

Reference	Optimisation type	Spatial scope	Spatial resolution	Temporal scope	Electricity sources	Hydrogen production	Hydrogen transport modes	Hydrogen demand sectors
Parker et al. (2010)	NLP	California, USA	5 nodes prod, 29 nodes dem	N/A	N/A	BG	GH2 trucks, LH2 trucks, rail, pipelines	HRS
Konda et al. (2011) [25]	MILP	The Netherlands	25 nodes	2015–2050, divided in 4 time periods	N/A	SMR, CG, BG, EL	GH2 trucks, LH2 trucks, pipelines	HRS
André et al. (2014) [29]	NLP	Northern France	26 nodes	2010–2050, 5-year timesteps	WPP mentioned, not analysed	SMR, HT-EL mentioned, but not analysed	GH2 trucks, LH2 trucks, pipelines	HRS
De-León (2014) [26]	MILP	Midi-Pyrénées, France	22 nodes	2020–2050, 10-year timesteps	PV, WPP, HP, Nuclear	SMR, EL	LH2 trucks	HRS
De-León (2015) [27]	MILP	France	21 nodes	2020–2050, 10-year timesteps	PV, WPP, HP, Nuclear	SMR, EL, BG	LH2 trucks	HRS
Talebian et al. (2019) [30]	MILP	British Columbia, Canada	varying	2020–2050, yearly timesteps	HP	SMR, EL, by-product	GH2 trucks, LH2 trucks	HRS
Cantú et al. (2023) [32]	MILP + NLP	Midi-Pyrénées, France	8 and 22 nodes	2020–2050, up to 7 timesteps	PV, WPP	SMR, EL	GH2 trucks	N/A

(*continued on next page*)

Appendix Table 1 (*continued*)

Reference	Optimisation type	Spatial scope	Spatial resolution	Temporal scope	Electricity sources	Hydrogen production	Hydrogen transport modes	Hydrogen demand sectors
Forghani et al. (2023) [31]	MILP	Oman	40 nodes	10 years	N/A	BG, CG, SMR, EL	GH2 trucks, pipelines	N/A
Guzzini er al (2023) [34]	NLP	Italy	40 km^2 grid	2030, 2050	PV, grid electricity	EL	GH2 trucks	HRS
Li et al. (2023) [33]	MILP	Dalian, China	9 nodes	2025, 2030, 2035	WPP, HP	BG, CG, SMR, EL	GH2 trucks, LH2 trucks	HRS
Pérez-Uresti et al. (2023) [36]	NLP	California, USA	4 nodes	2023–2032	grid	BG, CG, SMR, EL	GH2 trucks, LH2 trucks	HRS, industry
Cutore et al. (2024) [35]	MILP	Sicily, Italy	9 nodes	representative day	WPP	EL	GH2 trucks, LH2 trucks	HRS

Abbreviations can be found below the next appendix table.

Appendix Table 2
Relevant previous studies in which dynamic optimisation models for hydrogen supply chains have been applied.

Reference	Optimisation type	Spatial scope	Spatial resolution	Temporal scope	Temporal resolution	Electricity sources	Hydrogen production	Hydrogen transport modes	Hydrogen demand sectors
He et al. (2021) [37]	LP / MILP	USA North-East	6 nodes	20 representative weeks	hourly	grid	SMR, EL	GH2 trucks, LH2 trucks, pipelines	HRS
Parolin et al (2022) [39]	MILP	Sicily, Italy	98 nodes	2050	daily	PV	SMR, EL	GH2 trucks, LH2 trucks, pipelines	HRS
Wang et al (2022) [38]	MILP	Artificial bus systems	6 nodes, 118 nodes	representative weeks	hourly for electricity, daily for hydrogen	WPP, grid	SMR, EL	GH2 trucks, LH2 trucks, pipelines	N/A
Genovese et al. (2024) [40]	only simulation	Calabria, Italy	1 node prod, 7 node dem	unspecified year	daily	grid	EL	rail	HRS, maritime, aviation
Rosén et al. (2024) [41]	MILP	Swedish West Coast	3 nodes	2050	hourly	PV, offshore WPP, FC, thermal power plants	EL	pipelines	industry

Abbreviations: MILP – mixed-integer linear problem, NLP – nonlinear problem, prod – production, dem – demand, PV – photovoltaics, WPP – wind power plant, HP – hydropower, BG – biomass gasification, CG – coal gasification, SMR – steam methane reforming, EL – electrolysis, GH2 – gaseous hydrogen, LH2 – liquefied hydrogen, HRS – hydrogen refuelling stations, FC – fuel cell, NG – natural gas, BHM – biological hydrogen methanation

Data availability

Data will be made available on request.

References

[1] IEA. Global hydrogen review 2022. License: CC BY 4.0. Paris; 2022.
[2] Bampaou M, Panopoulos KD. An overview of hydrogen valleys: current status, challenges and their role in increased renewable energy penetration. Renew Sustain Energy Rev 2025;207:114923.
[3] Clean Hydrogen Partnership. Hydrogen Valleys. [April 17, 2023]; available from: https://h2v.eu/hydrogen-valleys.
[4] Satyapal S, Rustagi N, Green T, Melaini M, Penev M, Koleva M. U.S. National clean hydrogen strategy and roadmap; 2023.
[5] DCCEEW. *National hydrogen strategy* 2024. Canberra; 2024.
[6] Government of Canada. Hydrogen strategy for canada: seizing the opportunities for hydrogen. A call to action; 2020.
[7] Bundesministerium für Wirtschaft und Klimaschutz. Fortschreibung der Nationalen Wasserstoffstrategie; 2023.
[8] France Hydrogene. National hydrogen strategy: harnessing the hydrogen sector's full potential in pursuit of France's decarbonization and reindustrialization; 2023.
[9] Ministerio para la Transición Ecológica y el Reto Demográfico (MITERD). *Hoja de Ruta del Hidrogeno: Una Apuesta por el Hidrogeno Renovable*; 2020.
[10] CSWW - cross-sectorale werkgroep waterstof. Werkplan Nationaal Waterstof Programma 2022-2025; 2021.
[11] Uwe Weichenhain, Markus Kaufmann, Roland Berger (Anja Benz), *Guillermo Matute Gomez (Inycom)*. Hydrogen valleys: insights into the emerging hydrogen economies around the world 2021.
[12] Hörsch J, Hofmann F, Schlachtberger D, PyPSA-Eur Brown T. An open optimisation model of the European transmission system. Energy Strat Rev 2018;22:207–15.
[13] Henning H-M, Palzer A. A comprehensive model for the German electricity and heat sector in a future energy system with a dominant contribution from renewable energy technologies—Part I: methodology. Renew Sustain Energy Rev 2014;30:1003–18.
[14] Balyk O, Andersen KS, Dockweiler S, Gargiulo M, Karlsson K, Næraa R, et al. TIMES-DK: Technology-rich multi-sectoral optimisation model of the Danish energy system. Energy Strat Rev 2019;23:13–22.
[15] Limpens G, Moret S, Jeanmart H, Maréchal F. EnergyScope TD: A novel open-source model for regional energy systems. Appl Energy 2019;255:113729.
[16] Aryanpur V, O'Gallachoir B, Dai H, Chen W, Glynn J. A review of spatial resolution and regionalisation in national-scale energy systems optimisation models. Energy Strategy Reviews 2021;37:100702.
[17] van Stralen JNP, Dalla Longa F, Daniëls BW, Smekens KEL, van der Zwaan B. OPERA: a new high-resolution energy system model for sector integration research. Environ Model Assess 2021;26(6):873–89.
[18] Sahoo S, van Stralen JN, Zuidema C, Sijm J, Yamu C, Faaij A. Regionalization of a national integrated energy system model: a case study of the northern Netherlands. Appl Energy 2022;306:118035.
[19] Sahoo S, van Stralen JN, Zuidema C, Sijm J, Faaij A. Regionally integrated energy system detailed spatial analysis: groningen Province case study in the northern Netherlands. Energy Convers Manag 2023;277:116599.
[20] BALL M, WIETSCHEL M, RENTZ O. Integration of a hydrogen economy into the German energy system: an optimising modelling approach. Int J Hydrogen Energy 2007;32(10-11):1355–68.
[21] Welder L, Ryberg D, Kotzur L, Grube T, Robinius M, Stolten D. Spatio-temporal optimization of a future energy system for power-to-hydrogen applications in Germany. Energy 2018;158:1130–49.
[22] Hou P, Enevoldsen P, Eichman J, Hu W, Jacobson MZ, Chen Z. Optimizing investments in coupled offshore wind -electrolytic hydrogen storage systems in Denmark. J Power Sourc 2017;359:186–97.
[23] Terlouw T, Bauer C, McKenna R, Mazzotti M. Large-scale hydrogen production via water electrolysis: a techno-economic and environmental assessment. Energy Environ Sci 2022;15(9):3583–602.

[24] Petrollese M, Concas G, Lonis F, Cocco D. Techno-economic assessment of green hydrogen valley providing multiple end-users. Int J Hydrogen Energy 2022;47(57):24121–35.
[25] Murthy Konda N, Shah N, Brandon NP. Optimal transition towards a large-scale hydrogen infrastructure for the transport sector: the case for the Netherlands. Int J Hydrogen Energy 2011;36(8):4619–35.
[26] De-León Almaraz S, Azzaro-Pantel C, Montastruc L, Domenech S. Hydrogen supply chain optimization for deployment scenarios in the Midi-Pyrénées region, France. Int J Hydrogen Energy 2014;39(23):11831–45.
[27] De-León Almaraz S, Azzaro-Pantel C, Montastruc L, Boix M. Deployment of a hydrogen supply chain by multi-objective/multi-period optimisation at regional and national scales. Chem Eng Res Design 2015;104:11–31.
[28] Parker N, Fan Y, Ogden J. From waste to hydrogen: An optimal design of energy production and distribution network. Logist Transport Rev 2010;46(4):534–45.
[29] André J, Auray S, Wolf D de, Memmah M-M, Simonnet A. Time development of new hydrogen transmission pipeline networks for France. Int J Hydrogen Energy 2014;39(20):10323–37.
[30] Talebian H, Herrera OE, Mérida W. Spatial and temporal optimization of hydrogen fuel supply chain for light duty passenger vehicles in British Columbia. Int J Hydrogen Energy 2019;44(47):25939–56.
[31] Forghani K, Kia R, Nejatbakhsh Y. A multi-period sustainable hydrogen supply chain model considering pipeline routing and carbon emissions: The case study of Oman. Renew Sustain Energy Rev 2023;173:1–20.
[32] Cantú VH, Ponsich A, Azzaro-Pantel C, Carrera E. Capturing spatial, time-wise and technological detail in hydrogen supply chains: A bi-level multi-objective optimization approach. Appl Energy 2023;344:121159.
[33] Li M, Ming P, Huo R, Mu H, Zhang C. Optimizing design and performance assessment of a sustainability hydrogen supply chain network: A multi-period model for China. Sustain Cities Soc 2023;92:104444.
[34] Guzzini A, Brunaccini G, Aloisio D, Pellegrini M, Saccani C, Sergi F. A new geographic information system (GIS) tool for hydrogen value chain planning optimization: application to Italian highways. Sustainability 2023;15(3):2080.
[35] Cutore E, Fichera A, Inturri G, Le Pira M, Volpe R. Spatially-explicit optimization of an integrated wind-hydrogen supply chain network for the transport sector: The case study of Sicily. Int J Hydrogen Energy 2024;52:761–74.
[36] Pérez-Uresti SI, Gallardo G, Varvarezos DK. Strategic investment planning for the hydrogen economy – A mixed integer non-linear framework for the development and capacity expansion of hydrogen supply chain networks. Comput Chem Eng 2023;179:108412.
[37] He G, Mallapragada DS, Bose A, Heuberger CF, Gencer E. Hydrogen supply chain planning with flexible transmission and storage scheduling. IEEE Trans Sustain Energy 2021;12(3):1730–40.
[38] Wang S, Bo R. Joint planning of electricity transmission and hydrogen transportation networks. IEEE Trans. on Ind. Applicat. 2022;58(2):2887–97.
[39] Parolin F, Colbertaldo P, Campanari S. Development of a multi-modality hydrogen delivery infrastructure: An optimization model for design and operation. Energy Convers Manag 2022;266:115650.
[40] Genovese M, Piraino F, Fragiacomo P. 3E analysis of a virtual hydrogen valley supported by railway-based H2 delivery for multi-transportation service. Renew Sustain Energy Rev 2024;191:114070.
[41] Rosén S, Göransson L, Taljegård M, Lehtveer M. Modeling of a “Hydrogen Valley” to investigate the impact of a regional pipeline for hydrogen supply. Front Energy Res 2024;12.
[42] Holst M, Wunsch A, Jacobs J, Mendler F, Voglstätter C. Techno -economic analysis of renewable hydrogen production using a hydrogen process simulation (H2prosim) model. Manuscr Submitt Public.
[43] Guo D. Regionalization with dynamically constrained agglomerative clustering and partitioning (REDCAP). Int J Geographic Info Sci 2008;22(7):801–23.
[44] Mendler F, Koch B, Meißner B, Voglstätter C, Smolinka T. Evaluation of spatial clustering methods for regionalisation of hydrogen ecosystems. Manuscr Submitt Public 2024.
[45] Joint Research Center. *Photovoltaic geographic information system: european commission*. [April 17, 2023]; Available from: https://re.jrc.ec.europa.eu/pvg_tools/en/.
[46] Bundesnetzagentur. SMARD Strommarktdaten: Großhandelspreise. [March 28, 2024]; available from: https://www.smard.de.
[47] Hansen N, Auger A, Ros R, Finck S, Pošík P. Comparing results of 31 algorithms from the black-box optimization benchmarking BBOB-2009. In: Pelikan M, Branke J, editors. Proceedings of the 12th annual conference companion on Genetic and evolutionary computation. ACM; 2010. p. 1689–96.
[48] Hansen N. The CMA evolution strategy: a tutorial; 2016.
[49] Hansen N, Ostermeier A. Adapting arbitrary normal mutation distributions in evolution strategies: the covariance matrix adaptations. In: Proceedings of the 1996 IEEE international conference on evolutionary computation, p. 312–317.
[50] Jürgens P, Müller P, Brandhuber F, Kost C. Simulation-based optimization as a method for dealing with complexity in energy system modeling; 2024.
[51] Hansen N. The CMA evolution strategy. [May 03, 2024]; available from: https://cma-es.github.io/.
[52] Zipf A, Schönberger G. Openrouteservice: QGIS plugin; available from: https://github.com/GIScience/orstools-qgis-plugin.
[53] Milella V, Nachbar B, Kelly A, Lieske S, Bude S, Bayer T et al. Potenzialbeschreibung Wasserstofftransport über das Schienennetz; 2020.
[54] Gupta R, Basile A, Veziroglu N. Hydrogen storage, distribution and infrastructure. Amsterdam, Heidelberg: Elsevier; 2016.
[55] Mischner J. Zur frage der strömungsgeschwindigkeit in gasleitungen. Fachberichte Erdgas; 2021.
[56] Siala K, Mahfouz MY. Impact of the choice of regions on energy system models. Energy Strat Rev 2019;25:75–85.
[57] Klimapartner Oberrhein. Wasserstofftechnologien am südlichen oberrhein (H2-SO). [September 28, 2023]; available from: https://www.klimaschutz-oberrhein.de/de-de/projekte/wasserstofftechnologien_am_suedlichen_oberrhein-h2-so.
[58] Neuwirth M, Fleiter T, Manz P, Hofmann R. The future potential hydrogen demand in energy-intensive industries - a site-specific approach applied to Germany. Energy Convers Manag 2022;252:115052.
[59] Ostbayerische Technische Hochschule Regensburg. Wasserstoffatlas D. [July 18, 2024]; Available from: https://wasserstoffatlas.de/.
[60] s EEnergies. sEEnergies Open data: D5_1 industry dataset with demand data. [July 18, 2024]; available from: https://s-eenergies-open-data-euf.hub.arcgis.com/search?categories=%252Fcategories%252Fseenergies_industry.
[61] Umweltbundesamt. Pollutent Release and Transfer Register. [July 18, 2024]; Available from: https://thru.de/en/thrude/downloads/.
[62] VCI Verband der Chemischen Industrie e.V. List of Chemical Parks. [July 18, 2024]; available from: https://chemicalparks.com/chemical-parks/list-of-chemical-parks.
[63] Behrens J. PoWerD – Atlas über geeignete standorte für power-to-hydrogen-anlagen in deutschland. [July 18, 2024]; Available from: https://www.ise.fraunhofer.de/de/forschungsprojekte/powerd.html.
[64] Fleiter T, Fragoso J, Lux B, Alibaş Ş, Al-Dabbas K, Manz P, et al. Hydrogen infrastructure in the future CO 2 -neutral european energy system—how does the demand for hydrogen affect the need for infrastructure? Energy Tech 2024.
[65] Eurostat. NUTS - Nomenclature of territorial units for statistics; available from: https://ec.europa.eu/eurostat/web/nuts/.
[66] Eißler T, Schumacher G, Behrens J, Mendler F, Voglstätter C. Detailed cost analysis of hydrogen refueling costs for fleets. Chemie Ingenieur Technik 2024;96(1-2):86–99.
[67] Agora energiewende, reiner lemoine institut. Photovoltaik- und Windflächenrechner; available from: https://www.agora-energiewende.de/service/pv-und-windflaechenrechner/.
[68] Bundesnetzagentur. Marktstammdatenregister: Aktuelle Einheitenübersicht. Stromerzeugungseinheiten. [April 17, 2023]; available from: https://www.marktstammdatenregister.de/MaStR/Einheit/Einheiten/OeffentlicheEinheitenuebersicht.
[69] Navarrate A, Zhou Y. The price of green hydrogen: How and why we estimate future production costs. [October 04, 2024]; Available from: https://theicct.org/the-price-of-green-hydrogen-estimate-future-production-costs-may24/.
[70] Clean Hydrogen Partnership. Hydrogen valleys. [January 01, 2025]; available from: https://www.clean-hydrogen.europa.eu/get-involved/hydrogen-valleys_en.
[71] Department of Energy. *Regional clean hydrogen hubs selections for award negotiations*. [January 01, 2025]; available from: https://www.energy.gov/oced/regional-clean-hydrogen-hubs-selections-award-negotiations.
[72] Hydrogen and Fuel Cell Technologies Office. H2 matchmaker. [January 01, 2025]; available from: https://www.energy.gov/eere/fuelcells/h2-matchmaker.